

AD-A144 874

IMPLANTATION OF IONIZED MONOMER INTO ALUMINUM ALLOY
6061 FOR MARINE CORRO. (U) DAVID W TAYLOR NAVAL SHIP
RESEARCH AND DEVELOPMENT CENTER BET.

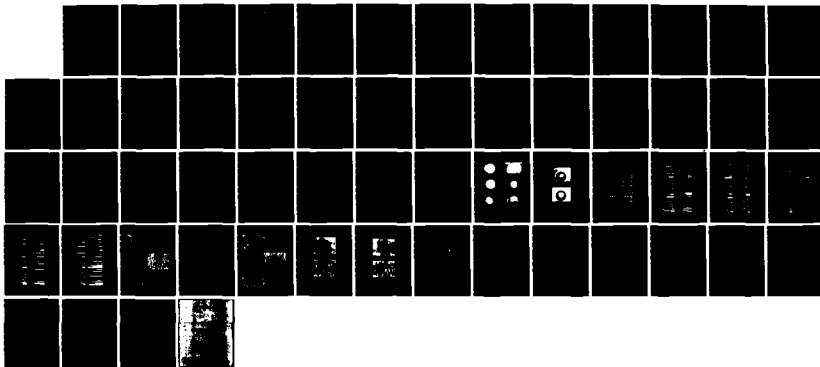
1/1

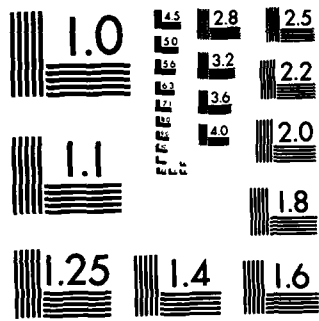
UNCLASSIFIED

S R TAYLOR ET AL. JUL 84 DTNSRDC-84/046

F/G 13/8

NL





MICROCOPY RESOLUTION TEST CHART
NATIONAL BUREAU OF STANDARDS-1963-A

DTNSRDC-84/046

IMPLANTATION OF IONIZED MONOMER INTO ALUMINUM ALLOY 6061 FOR MARINE CORROSION PROTECTION

18

DAVID W. TAYLOR NAVAL SHIP RESEARCH AND DEVELOPMENT CENTER

Bethesda, Maryland 20084



IMPLANTATION OF IONIZED MONOMER INTO ALUMINUM ALLOY 6061 FOR MARINE CORROSION PROTECTION

by

S.R. Taylor, G.L. Cahen, Jr., and G.E. Stoner
Applied Electrochemistry Laboratory
Department of Materials Science
University of Virginia

and

P.J. Moran
David Taylor Naval Ship R&D Center

and

M.W. Ferralli
Department of Physics
Gannon University
Erie, Pennsylvania

AUG 24 1984

AD-A144 874

DTIC FILE COPY

APPROVED FOR PUBLIC RELEASE: DISTRIBUTION UNLIMITED

SHIP MATERIALS ENGINEERING DEPARTMENT
RESEARCH AND DEVELOPMENT REPORT

July 1984

DTNSRDC-84/046

84 08 24 002

UNCLASSIFIED

SECURITY CLASSIFICATION OF THIS PAGE (When Data Entered)

REPORT DOCUMENTATION PAGE		READ INSTRUCTIONS BEFORE COMPLETING FORM
1. REPORT NUMBER DTNSRDC-84/046	2. GOVT ACCESSION NO. AD A244 874	3. RECIPIENT'S CATALOG NUMBER
4. TITLE (and Subtitle) IMPLANTATION OF IONIZED MONOMER INTO ALUMINUM ALLOY 6061 FOR MARINE CORROSION PROTECTION		5. TYPE OF REPORT & PERIOD COVERED
		6. PERFORMING ORG. REPORT NUMBER
7. AUTHOR(s) S.R. Taylor, G.L. Cahen, Jr., and G.E. Stoner; and P.J. Moran; and M.W. Ferralli		8. CONTRACT OR GRANT NUMBER(s)
9. PERFORMING ORGANIZATION NAME AND ADDRESS David W. Taylor Naval Ship Research and Development Center Bethesda, Maryland 20084		10. PROGRAM ELEMENT, PROJECT, TASK AREA & WORK UNIT NUMBERS Program Element 62761N Task S0154001 Work Unit 2813-420
11. CONTROLLING OFFICE NAME AND ADDRESS		12. REPORT DATE July 1984
		13. NUMBER OF PAGES 56
14. MONITORING AGENCY NAME & ADDRESS (if different from Controlling Office)		15. SECURITY CLASS. (of this report) UNCLASSIFIED
		15a. DECLASSIFICATION/DOWNGRADING SCHEDULE
16. DISTRIBUTION STATEMENT (of this Report) APPROVED FOR PUBLIC RELEASE: DISTRIBUTION UNLIMITED		
17. DISTRIBUTION STATEMENT (of the abstract entered in Block 20, if different from Report)		
18. SUPPLEMENTARY NOTES		
19. KEY WORDS (Continue on reverse side if necessary and identify by block number) Aluminum 6061-T6 Alloy Polymer Implantation Corrosion Protection Protective Coating Ion Implantation Surface Modification Pitting Corrosion		
20. ABSTRACT (Continue on reverse side if necessary and identify by block number) Ion implantation technology has been extended to include the ionization of monomer gases and their subsequent acceleration and implantation into metallic and other substrates. The variables and options involved in the process are numerous and are discussed in the report. The resulting thin films are polymeric in nature and possess no traditional interface with the substrate, thus improving adhesion. The purpose of this study is to investigate (Continued on reverse side)		

DD FORM 1 JAN 73 1473

EDITION OF 1 NOV 55 IS OBSOLETE
S/N 0102-LF-014-6601

UNCLASSIFIED

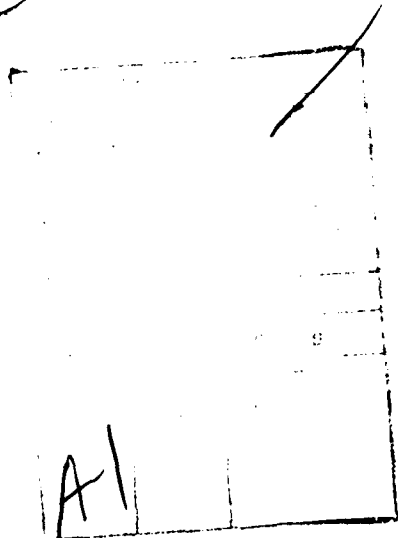
SECURITY CLASSIFICATION OF THIS PAGE (When Data Entered)

UNCLASSIFIED

SECURITY CLASSIFICATION OF THIS PAGE (When Data Entered)

(Block 20 continued)

these ion-beam-related film formation techniques for their ability to protect 6061-T6 aluminum alloy from corrosion attack in natural seawater. Improved resistance to pitting corrosion was observed for several of the treatments tested. The best resistance to pitting was produced by the following treatment: a 30-keV hydrogen ion beam is directed through a butadiene collisional gas with a 13.6-V/cm field applied to the substrate. This treatment is believed to promote hydrocarbon polymerization, resulting in a thin film possessing increased adhesion and film integrity. It should be re-emphasized that the purpose of this investigation was to screen a number of possible treatments for protection of one alloy in seawater. The positive results will hopefully encourage broader experimentation with this unique and potentially very useful technology.



UNCLASSIFIED

SECURITY CLASSIFICATION OF THIS PAGE (When Data Entered)

TABLE OF CONTENTS

	Page
LIST OF FIGURES	iii
LIST OF TABLES	iv
ABBREVIATIONS	v
ABSTRACT	1
ADMINISTRATIVE INFORMATION	1
INTRODUCTION	2
EXPERIMENTAL METPODS	4
SAMPLE PREPARATION	4
SEAWATER IMMERSION	9
PITTING QUANTIFICATION	10
RESULTS	11
MACROSCOPIC EXAMINATION	12
PITTING QUANTIFICATION	13
DISCUSSION	17
EFFECT OF ION IMPLANTATION ON THE SUBSTRATE	18
THE METAL/FILM INTERFACE	20
THE FILM	21
CONCLUSION	22
SUGGESTED FUTURE WORK	23
REFERENCES	47

LIST OF FIGURES

1 - Implantation Modes	24
2 - Schematic of Ion Implantation Device	25
3 - Differentially Pumped Collisional Cas Chamber	26

	Page
4 - Sampling Schemes Used to Assess Specimen Corrosion	27
5 - Appearance of Typical Sample Treatments and Control Specimen Before Corrosion Testing (1-in.-diam discs)	28
6 - Sample Treatment 4 After 120 Days of Seawater Immersion	29
7 - Percent Pitted Area for 30-Day Exposure	30
8 - Pit Depth Mode for 30-Day Exposure	31
9 - Maximum Pit Depth for 30-Day Exposure	32
10 - Percent Pitted Area for 120-Day Exposure	33
11 - Pit Depth Mode for 120-Day Exposure	34
12 - Maximum Pit Depth for 120-Day Exposure	35
13 - Sample Treatment 1 After 120-Day Exposure	36
14 - Typical Pitting on Sample Treatment 2 After 120-Day Exposure (450X)	37
15 - Sample Treatment 3 After 120-Day Exposure	38
16 - Sample Treatment 4 After 120-Day Exposure	39
17 - Sample Treatment 5 After 120-Day Exposure	40
18 - Control After 120-Day Exposure	41

LIST OF TABLES

1 - Summary of Sample Treatments	42
2 - Comparison of Sample Treatments as to Average Percent Pitted Areas after Two Immersion Periods	42
3 - Comparison of Average Pit Depth Mode	43
4 - Comparison of Maximum Pit Depth	43
5 - Comparison of Average Pitting Parameters (UVAPPs)	44
6 - Ranking of Overall Performance of Sample Treatments	45
7 - Refined Ranking of Overall Performance of Sample Treatments	45

ABBREVIATIONS

A	Angstrom
Al	Aluminum
C	Carbon
cm	Centimeter
diam	Diameter
eV	Electron volts
H	Hydrogen
H ⁺	Ionized hydrogen
ISS	Ion Scattering Spectroscopy
keV	Thousands of electron volts
l	Liter
m	Meter
Mohm	Megaohm
s	Second
SIMS	Secondary Ion Mass Spectroscopy
UVAPP	University of Virginia Pitting Parameter
V	Volts
μ	Micron (10 ⁻⁶ meter)
μamp	Microamperes

ABSTRACT

Ion implantation technology has been extended to include the ionization of monomer gases and their subsequent acceleration and implantation into metallic and other substrates. The variables and options involved in the process are numerous and are discussed in the report. The resulting thin films are polymeric in nature and possess no traditional interface with the substrate, thus improving adhesion. The purpose of this study is to investigate these ion beam-related film formation techniques for their ability to protect 6061-T6 aluminum alloy from corrosion attack in natural seawater. Improved resistance to pitting corrosion was observed for several of the treatments tested. The best resistance to pitting was produced by the following treatment: a 30-keV hydrogen ion beam is directed through a butadiene collisional gas with a 13.6-V/cm field applied to the substrate. This treatment is believed to promote hydrocarbon polymerization, resulting in a thin film possessing increased adhesion and film integrity. It should be re-emphasized that the purpose of this investigation was to screen a number of possible treatments for protection of one alloy in seawater. The positive results will hopefully encourage broader experimentation with this unique and potentially very useful technology.

ADMINISTRATIVE INFORMATION

The ionized monomer implantation technique was tested as a potential corrosion control method for aluminum. The program was sponsored by the Naval Sea Systems Command. Treatment of the specimens was contracted to the University of Virginia and to Gannon University. Corrosion testing was done by the Marine Corrosion Branch of this Center in cooperation with the LaQue Center for Corrosion Technology. The pitting analysis was also conducted at the University of Virginia.

INTRODUCTION

The application of ion beams and plasmas to modify the surface and near-surface properties of materials has gained recognition as a potentially diverse and useful tool in the materials sciences. The control of ion species/substrate combinations and ion energies has been utilized extensively as a method of doping semiconductors,^{1*,2} as well as improving tribological properties,^{3,4} metal film adhesion,⁵ and corrosion resistance.^{6,7} By controlling ion energies and ion fluences, one can deposit thin films, implant atoms below the surface, or form films which extend into the substrate on an atomic scale.

Thin-film formation techniques utilizing low-energy ion plasmas (≈ 100 eV**) include ion beam sputter coating,⁸ and ion beam plating.⁸⁻¹⁰ The relatively low energies used in these techniques provide sufficient kinetic energy for thin-film nucleation and growth but do not allow for subsurface implantation. These low-energy processes have the capability of depositing metallic, insulating (polymeric), and semiconducting films on any solid substrate.

Ion implantation, however, is a process by which high-velocity ions can be injected into the near-surface region of a solid substrate using accelerating voltages ranging from tens to hundreds of kilovolts. High-energy ions (> 100 keV) are able to penetrate to depths of thousands of angstroms before collisions with substrate atoms dissipate the kinetic energy of the incident ion.¹¹ Depth profiles can be produced with a high degree of controllability and reproducibility and have been calculated for a large number of implant species/host combinations.¹²

The nonequilibrium nature of ion implantation has the potential to overcome the limitations imposed by equilibrium phase concentrations. Thus, components can be alloyed in concentrations beyond normal solubility limits, and solid solutions of components which are normally immiscible using conventional alloying techniques can be produced. Consequently, one can create novel, metastable, single-phase, surface alloys without altering desirable bulk properties.

*A complete listing of references is given on page 47.

**Definitions of abbreviations used are given on page v.

Until recently, all ion implantation processes have used pure elements (solids or gases) as the implant species. The technique of ion implantation has been extended into a new technology involving the ionization, beam formation, acceleration (10-100+ keV), and implantation of monomer gases (e.g., ethylene and butadiene).¹³ Two basic implantation procedures have been used: (a) the direct ionization, beam formation, and implantation of a monomer gas, and (b) implantation via a collisional process whereby an ion beam of either an elemental (e.g., H^+) or monomeric (e.g., ethylene) species is directed into a monomeric target gas in front of the substrate (Figure 1). The result of these processes is a thin (50-500A) organic film whose elemental constituents (C and H) have been implanted in the near-surface region of the target (metal, glass, polymer) as demonstrated by ISS (Ion Scattering Spectroscopy) and SIMS (Secondary Ion Mass Spectroscopy).¹⁴

One of the unique advantages of this thin-film formation technique is the enhancement of film adhesion, an important aspect of thin-film protection. In the ideal case of monomer implantation, the atomic constituents of the polymer film are integrated into the substrate on an atomic level, thus eliminating the concept of a classical interface as associated with other coating techniques. Even if there is deviation from the ideal, there will be points of strong bonding between the C in the film and the C implanted in the near-surface region of the target.

The purpose of this study is to investigate these ion-beam-related film formation techniques for their ability to protect the lightweight aluminum alloy 6061-T6 in a seawater immersion test. Due to the large number of processing techniques (elemental beam only, monomer beam only, elemental beam into monomer, monomer beam into monomer, etc.) and process variables (accelerating voltage, time, beam gas, collisional gas, etc.) a series of five treatments was selected (Table 1). A two-fold rationale was used for process selection: Some processes were intuitively chosen on the basis of offering the best corrosion resistance, while other processes were chosen for experimental verification.

EXPERIMENTAL METHODS

SAMPLE PREPARATION

Sixty five circular discs (2.5 cm diam \times 0.3 cm thick) of 6061-T6 aluminum alloy were cut from standard sheet. The discs were prepared using this sequence: (a) thorough cleaning with reagent-grade hexane, (b) polishing with 500 grit sandpaper to remove machining marks, (c) hand polishing with 0.1-micron (μ) aluminum oxide in water, and (d) a final hexane cleaning. Samples which were to be processed by irradiation treatment remained immersed in hexane to assure the absence of undetermined hydrocarbon contamination which might polymerize upon irradiation and invalidate any conclusions drawn from the experiment. The samples were divided into six sets. Five sets containing eleven specimens each were prepared for various irradiation treatments, and one set of ten specimens was prepared to serve as a reference. All sample sets were kept under identical conditions until subjected to the irradiation treatment, and all samples within a set were irradiated as identically as possible. This procedure assured that any differences in surface properties noted between sets could be directly attributed to the irradiation treatment rather than to preirradiation handling. However, it must be noted that some variability within a sample set was expected due to the extreme difficulty in sustaining constant radiation parameters.

The irradiation treatments described below were undertaken at the State University of New York, College at Fredonia, Particle Accelerator Facility. The accelerator is a Cockcroft-Walton 150-keV neutron generator which was modified to function as an ion implantation device (Figure 2). The modified accelerator can produce ion beams of any material having a room temperature vapor pressure of greater than 50 μ . The beams have energies up to 150 keV with an energy spread of approximately 100 eV. The ion beam can be focused from a 2-mm to a 2.5-cm-diam spot on a sample using a gap lens and focusing electrode combination. The ions are produced by a radio-frequency glow discharge which yields almost totally singly ionized species. Vacuum is achieved in the accelerator by means of a 4-in. oil diffusion pump system, with a

rating of 700 l/s , to produce a static vacuum in the low $0.0001\text{-}\mu$ range and an operating vacuum in the $0.001\text{-}\mu$ range. Hydrocarbon contamination from the oil diffusion system is minimized by the inclusion of a water-cooled baffle mounted directly over the vacuum pump assembly. Attached to the end of the accelerator is a gas cell consisting of a 10.6-cm -long, 4.13-cm -internal-diam pyrex glass tube capped at both ends by electrically isolated aluminum housings. The cell is shown in Figure 3. One of the aluminum housings contains an indentation for holding the appropriate specimens, while the other holds two tantalum discs with 0.5-cm -diam holes drilled into their centers. As shown in Figure 3, the discs are positioned so that the holes are aligned and form an aperture which allows the entry of the ion beam while permitting containment of any gas or material in the vapor phase. It was experimentally found that pressures of 200μ could be maintained within the gas cell when the accelerator was operated below a $0.05\text{-}\mu$ threshold. As shown in this figure, the gas cell contains an inlet for a gas or material in vapor phase. Control of gas flow into the gas cell, and thus control of the gas cell pressure, is accomplished by means of a thermomechanical leak valve attached to this gas cell inlet. An electric field could be produced and maintained within the gas cell simply by creating a potential difference between the aluminum housings.

Sample Set 1

Each of the specimens of Set 1 were irradiated using a hydrogen ion beam at an energy of 30 keV . No gas or electric field was present in the gas cell; however, due to the tantalum apertures, a 0.5-cm -diam spot on the samples was treated. Samples were irradiated until a charge of 0.0012 coulomb was delivered. Because of secondary electron emission produced by the hydrogen ions colliding with the samples, this charge can only give a crude approximation of the total number of ions arriving at the specimen. Therefore, approximately 7.5×10^{15} ions struck each sample. Irradiation treatment of Sample Set 1 was performed in order to determine whether or not the effects of a hydrogen ion beam alone would sufficiently alter the specimen surface so as to produce anticorrosion properties. It is known that ion irradiation of a surface will produce a number of alterations, including a

reduction of grain size, an increase in the number of surface dislocations and defects, an alteration of surface and near-surface elemental and molecular composition due to ion implantation and ion-induced chemical reactions, and changes in surface morphology due to both uniform and preferential sputtering and recoil reactions. All of the above effects can cause changes in the corrosion properties of a material. Corrosion testing of Sample Set 1 would determine the cumulative effect of all of these alteration processes in inhibiting corrosion.

Sample Set 2

Each of the specimens of Sample Set 2 were irradiated with an ion beam consisting of the products produced when ethylene is ionized using a radio-frequency-initiated glow discharge. The ion beam consists of singly ionized ethylene and all possible ionic fragments thereof, in unknown proportion (although it may be reasonable to assume that the principal ingredient of the beam is singly ionized ethylene), at an energy 30 keV. As in the irradiation treatment of Sample Set 1, no gas or electric field was present in the gas cell. However, in order to expose as much of the specimen as possible to the alteration process, the tantalum apertures were removed. The specimens were irradiated until a charge of 0.03 coulomb was delivered, and again, ignoring secondary electron emission effects as well as sputtered ion production, this charge represents delivery of 1.9×10^{17} ions. The irradiation treatment on Sample Set 2 would serve to determine the effects of hydrocarbon implantation and high-energy surface and near-surface interactions on corrosion inhibition as compared to that induced by a hydrogen ion beam. It is noted that the kinetic energy of the ethylene-derived ion beam far exceeds the binding energy of any bond in the ethylene molecule, so that it is reasonable to assume that such bonds would be destroyed in the ion/specimen collision. To a first approximation, irradiation of the specimen in this manner would be functionally equivalent to irradiation by a composite beam of carbon and hydrogen ions and molecules, the latter being inferred since an ion/specimen collision can produce neutral fragments and elements. The effects of the collision of this composite beam is manifold.

For example, the range in depth of the 30-keV carbon ions and elements in the specimen is far less than the range of equivalent energy hydrogen ions and elements, and their damage capability is far greater.¹² Thus the damage profile of this composite beam is expected to be distinctively different from that produced by the hydrogen ion beam, and all consequential reactions and alterations dependent upon the damage profile will be different. Further, there is evidence that a hydrocarbon ion beam impacting upon a specimen will create polymeric species on and in the specimen surface.* These species appear to be similar to a polymer which is merged with the specimen surface such that no clear boundary exists between the altered surface and the bulk material.

Sample Set 3

Each of the specimens of Sample Set 3 were irradiated using a hydrogen ion beam at an energy of 30 keV. 1,3 butadiene at a pressure of 60 μ was present in the gas cell, as was an electric field directed to the specimen. The electric field was established by grounding the apertures through a 9.1-Mohm resistance while essentially grounding the specimens. Since about 15 μ amps of the hydrogen ion beam inadvertently struck the apertures, the resistance assured that the apertures were typically 136 V above the specimen. Thus an electric field of about 13.6 V/cm directed toward the specimen existed in the gas cell. The specimens were irradiated until a charge of 0.015 coulomb was delivered. It is noted that this charge has a much more complex source than that delivered in either Sample Sets 1 or 2. This charge represents the sum of the hydrogen beam ions, the positive butadiene-derived ions, the sputtered ions, the electrons, and the negative ions arriving at or leaving the specimen. Ignoring negative charge contribution and sputtered ion effects, 9.4×10^{16} ions were delivered. Sample Set 3 was prepared in order to determine whether the net effects of a hydrogen ion beam and the electric-field-directed secondary butadiene ions produced therefrom would cause significant corrosion-inhibiting surface alterations. There is evidence that the above sample processing serves both to activate the specimen surface and to cause polymerization of the hydrocarbon in the gas cell preferentially onto the activated surface, resulting in increased adhesion and film integrity on the specimen.^{13,*}

*M.W. Ferralli, private communication (1983).

Sample Set 4

Each of the specimens of Sample Set 4 were irradiated in a manner and under conditions identical to those of Sample Set 3 until a charge of 0.003 coulomb was delivered. After such treatment, however, a potential of 1000 V was placed between the apertures and the specimen (the specimen being negative), and the irradiation was continued for an additional 5 minutes. In this additional processing, the configuration used did not allow measurement of the accumulated charge and/or current. The additional processing significantly differs from the treatment of Sample Set 3 in that the 100-V/cm electric field is large enough to produce a glow discharge in the gas cell wherein the ion/electron pairs are not only produced by the hydrogen ion beam but also by the directed electric field. The net effect of this treatment is to substantially increase the number of butadiene ions arriving at the specimen surface and thus significantly increase the rate of surface polymer film formation. Sample Set 4 was prepared to determine whether the additional coating would significantly enhance the corrosion resistance properties of the specimens.

Sample Set 5

Each of the specimens of Sample Set 5 were irradiated by an ethylene-derived ion beam similar to that used in the treatment of Sample Set 2. The gas in the gas cell was 1,3 butadiene at a pressure of 30 μ . The apertures were grounded through the 9.1-Mohm resistor, while the specimens were directly grounded, a configuration essentially similar to that used in processing Sample Sets 3 and 4. However, the reduced beam current resulted in an electric field of 9 V/cm. The gas cell pressure of 30 μ was used in order to stabilize accelerator conditions. As in the irradiation of Sample Set 4, an additional 5-minute processing was carried out in order to increase butadiene ion production which, consequently, increases the polymer film formation on the specimen surface. Sample Set 5 was prepared in order to determine whether changing the ion beam to one capable of creating hydrocarbon species within the specimen surface would significantly increase the corrosion resistance properties over those found in Sample Set 4.

Sample Set 6

In order to establish a basic corrosion reference, a set of ten specimens was prepared by cleaning and polishing, as previously outlined, but was not irradiated. The terms "Sample Set 6," "sample 6," and "control" will be used interchangeably.

SEAWATER IMMERSION

The previously described ion-beam-modified discs were tested by full immersion in quiescent, filtered, 30°C natural seawater and by exposure to marine atmosphere. Three nonconductive test panels (7.5×37.5×0.3 cm) were utilized. Each panel contained two specimens of each of the five ion beam surface treatments as well as two control samples (Sample Set 6). The sample discs (2.5×0.3 cm) were affixed to the test panels with General Electric RTV-108 Silicone Rubber. The perimeter of each disc, as well as the crevices between the disc and test panel, was coated with a stopoff lacquer (Tolber Microstop) to assure exposure of only the top flat surface of the samples.

The test panels were exposed at the LaQue Center for Corrosion Technology, Inc., Wrightsville Beach, N.C., facility. One panel was exposed for 31 days and a second for 120 days in full immersion. The seawater was replenished during testing by a slow-drip feed which did not disturb the quiescent conditions. The third panel is presently exposed at the Kure Beach 25-m lot. The third panel is intended to be a long-term exposure and will be analyzed after severe attack has been observed on the control specimens.

Once recovered, immersion samples were cleaned in two steps. Heavy macrofouling was removed by light brushing and flowing water. A second cleaning procedure used a warm chromic acid/phosphoric acid solution (ASTM G1-81) to remove corrosion products from the pit interiors. This provided better pit visibility for the quantification procedures.

PITTING QUANTIFICATION

Preliminary examination of corroded aluminum samples revealed minute pits (1-10 μ diam) in certain regions of the sample, as would be expected for a passive metal in a chloride environment. Since weight loss measurements are not very meaningful in the assessment of pitting corrosion, the amount and degree of pitting was quantified by three morphological features: (a) the percent of sample area covered by pits, (b) pit depth mode, and (c) maximum pit depth. Due to the small size of the pits, all measurements were made at a magnification of 400X on an inverted-stage metallograph (Zeiss Model ICM-405). At this magnification, a scan of the entire sample surface would be extremely laborious. This, in addition to the radial distribution of the beam energy (and, consequently, the surface treatment), necessitated a sampling system as shown in Figure 4. Two randomly selected radial scans were made on each sample, starting from the center of the beam-treated area and extending radially outward to the sample perimeter. The central frame was designated as "frame 1," and each subsequent frame could be counted as the microscope stage radially traversed the sample (Figure 4). Measurements were typically made on Frames 1, 5, 7, 10, 20, 30, 40, 50, 60, and 70. This sampling scheme was adhered to closely in order to eliminate sampling bias. A description of the three morphological features measured follows.

Percent Pitted Area

Some regions contained small numbers of individual pits and other regions contained large numbers of interconnecting pits. Therefore, measurements were made on the percentage of sample area covered by pits. Photographs were taken of each pre-designated frame of interest (i.e., 1, 5, 7, 10, etc.). By superimposing a regular grid over the photograph, a quantitative method of point counting can be used.¹⁴ The percent pitted area is proportional to the ratio of the number of grid intersections lying on pits to the total number of grid intersections. The grid was rotated in different directions so that four counts (an average of 1050 grid points) were made for each frame for increased accuracy.¹⁵ The data for corresponding frames from the two scans was averaged, and 95% confidence intervals were calculated according to Student's t-test.¹⁶

Pit Depth Mode

Pit depths could be measured by focusing the objective lens first on the sample surface, and then down into the pits, and noting the distance traversed during this focusing maneuver (indicated on the focusing knob). The units from the focusing knob were converted into micron units.

When focusing from the sample surface into the pits, a point is reached where the bottoms of a majority of the pits come into focus. This depth was recorded and designated as the "pit depth mode." The term "mode" rather than "average" is used because mode refers to the quantity within a distribution which occurs with the highest frequency.

Maximum Pit Depth

In any particular frame, there was a point where only one pit remained in focus as one was focusing down into the pits. This was recorded as the "maximum pit depth." The maximum pit depth is considered as one of the more important parameters in pitting corrosion. Therefore the data presented in Figures 9 and 12 represent the most severe pit depth for each frame and not the average of the two data points taken.

RESULTS

Marine immersion tests of 30 and 120 days were performed on these 6061-T6 aluminum alloy samples treated by the ion beam treatments outlined in Table 1 and described previously. For ease of discussion, the samples will be referred to by treatment number and the number of days in seawater. Thus, sample "3-30" refers to the sample with ion beam Treatment Number 3 and a 30-day marine immersion; sample "4-120" refers to Treatment Number 4 and a 120-day marine immersion.

MACROSCOPIC EXAMINATION

Prior to Seawater Immersion

All sample surfaces had small multidirectional scratches approximately 0.5-1.0 μ in width (Figure 5). Occasionally, larger (5-10 μ) scratches were observed. The proton beam treatment (Sample Set 1) was restricted to a circular area approximately 0.5 cm in diameter, displaced slightly offcenter, and appearing as a dark grey region. Sample Treatment 2 had a slightly discolored circular region 1.8 cm in diameter, but the sample was reflective over the entire surface. Sample Treatment 3 was similar in appearance to Treatment 1; however, the outside border of the treatment was diffuse, and discoloration gradually faded out within 0.5 cm from the treatment center. Treatment 4 contained a 1.6-cm-diam discolored region composed of concentric rings of varying density. Sample Treatment 5 was similar to Sample Treatment 3. There was a small dark (almost bluish) region of beam treatment which faded away gradually with distance from the center.

Post Immersion

Biofouling was evident on all sample surfaces after 31 days of immersion, and was considerable after 120 days. No effort was made to examine the extent of biofouling on the treated and untreated surface regions. Figure 6a shows Sample Treatment 4 after 120 days in seawater; Figure 6b is the same sample after the initial mechanical cleaning.

After Cleaning

An interesting result was observed following the chromic acid/phosphoric acid cleaning (ASTM-61-81). Film detachment was observed in the region outside of the 0.5-cm central beam area on Sample Treatments 3-5. These regions correspond to areas where plating of ionized monomer occurred. While Specimens 4 and 5 were in the cleaning solution, film separation was observed at the outer edges of the treated area. A visible film began to lift from the treatment area circumference, and the separation front moved radially inward with time. Film separation ceased at the perimeter of the ion beam irradiated region, suggesting an improved film adhesion as a result of ion beam treatment.

PITTING QUANTIFICATION

The pitting data (i.e., percent area, pit depth mode, and maximum pit depth) were plotted as a function of radial distance r from the center of the beam treatment (Figures 7-12). In general, two basic regions on the sample surfaces could be distinguished: a central beam-treated region ($0 < r < 2.0$ mm), and an outer region beyond the range of direct beam impact ($r > 2.0$ mm). The processing techniques were, therefore, assessed by comparing the data obtained from these two regions.

The data presented in Tables 2-5 were used to compare and rank the treatments. Table 2 compares the average percent pitted area for all treatments for the 30- and 120-day exposures. For Treatments 1, 3, 4, and 5 the data are displayed as beam area and outer area. Beam area refers to the 0- to 2.0-mm radius central region of direct beam impact, and outer area refers to the region from 2-mm radius out to the perimeter, excluding the edge. For Treatment 2, the distinction is not made because the treated area (beam-impacted area) for this treatment was essentially the entire surface. Also, no distinction is made for the control specimen. The average percent pitted area for the beam area is determined from four frames in each case, and five frames each were used to determine those of the outer areas. For Treatments 2 and 6, nine frames were utilized to determine the averages. These procedures were also employed in generating Tables 3-5.

Table 3 is a comparison of the average pit depth mode for all treatments for both the 30- and 120-day exposures. The data were averaged over the number of frames indicated above for each case, and the pit depth mode for each frame was determined as previously indicated.

Table 4 is a comparison of the maximum pit depth observed for each frame. These figures are not averages but represent the most severe pit depth.

A pitting parameter (Univ. of Virginia Pitting Parameter, or UVAPP) was defined for each frame. The UVAPP is the percent pitted area for the frame multiplied by the pit depth mode for the frame. This parameter is proportional to the volume lost due to pitting. In Table 5 a comparison of the average UVAPPs for all treatments at 30 and 120 days is shown. The distinctions and number of frames used to determine the averages are as previously described.

30-Day Immersion Tests

Percent Pitted Area. The data profiles for samples 1, 3, 4, and 5 reveal clear demarcations of the central beam area treatments (Figure 7). Sample 2 possessed uniform pit area coverage across the surface due to the absence of beam restriction by an aperture. The control sample (Sample 6) also displayed a uniform pit area profile, as one would expect.

Sample 1 (H^+ beam only) exhibited a unique phenomenon. The central beam area, which contained a low level of pit area, was surrounded by an annular region (≈ 0.1 cm wide) of intense corrosion. Moving out radially along the sample, the pit area diminished back to the low level observed in the beam area.

Samples 3-5 revealed low levels of pitting in the beam area with a gradual increase in the case of Samples 3 and 4 and a sharp increase in pit coverage in the case of Sample 5 as one moves to the perimeter of the sample. The high levels of pitting in the outer regions of these samples are associated with the ion-plated polymer films. In all cases (Samples 3-5), individual pits were seen in the central beam areas. Beyond 2000μ the pitting took on the appearance of interconnecting channels with few individual pits.

The beam-treated areas of all samples showed markedly reduced levels of pit area when compared to the control sample. The central region of Sample 4 displayed a level of pit coverage which was 4.4% that of the control. Sample 2, however, demonstrates a consistent level of pitting across the entire sample (30.1% that of the control).

Pit Depth Mode. Sample 1 displays a similar profile in the pit depth mode (Figure 8) as seen in the percent pit area (Figure 7). There is a low average pit depth in the beam-treated area which is surrounded by a band of increased corrosion.

No correlatable trends in pit depth data could be seen in Samples 2 and 6, and therefore the pit depths were considered to be constant across the entire specimens.

Samples 3-5 show a general level of increased pit depth in comparison to the control sample. The average pit depths are not reduced in the beam treated areas, and in Sample 4 they show marked increase. A general inverse relationship between pit area and pit depth mode can be seen in Sample 4.

The central beam area of Sample 1 demonstrated the best average pit depth (61.3% that of the control). However, it is unclear what effect the outer region has on the overall corrosion process with regards to cathodic protection by this highly corroding outer region.

Maximum Pit Depth. Sample 1 again displays the profile seen in the previous measurements (reduced central region with a ring of increased corrosion). The deepest pits were observed in the outer regions of all beam-treated samples with the exception of Sample 5 (Figure 9).

The data in Table 4 were obtained by considering the deepest pit in each of the respective regions (i.e., beam area vs. outer region). Sample 1 displays the best protection in the beam area as compared to the control, followed by 2, 3, 4, and 5, successively.

120-Day Immersion Test

Percent Pitted Area. The pit area profiles observed in the 30-day test samples (Figure 7) were essentially duplicated in the 120-day test samples (Figure 10). Any minor discrepancies in the beam area size were a result of cutting the samples away from the center line. The general level of corrosion as measured by pit area is increased in all samples at 120 days over the 30-day test.

A comparison of the beam-treated areas in Samples 1-5 to the control sample demonstrated a reduced pit area in all of the treated samples. Sample 3 reveals the best performance, followed by Samples 5, 4, 2, and 1. Figures 13-18 represent typical pitting observed in the major areas (central beam vs. outer area) of each sample after 120-day seawater immersion. Since no large differences were observed in pitting across Samples 2 and 6, only one figure is shown.

An equally important consideration of the data is that of kinetics. That is, one must look at the change in pitting measurements with respect to time. As an example, Table 2 shows a 588% increase in the pit area in the beam-treated region when comparing the 30- and 120-day data, while Sample 3 reveals no increase. These will be important considerations in the final assessment of the processing techniques.

Pit Depth Mode. Pit depth mode profiles for Samples 1, 2, and 6 for the 120-day exposure (Figure 11) were similar in shape to their respective 30-day profiles (Figure 8). In all cases except Sample 4, there is a general increase in the average pit depth at 120 days. The beam area of Sample 5 contained so few pits that any given field of view contained either one or no pits; consequently, a pit depth mode measurement was not applicable.

The beam areas of Samples 1-4 revealed depth modes which were 86%, 94%, 98%, and 125% respectively, that of the control value. However, the control (Sample 6) displayed the smallest increase in pit depth mode from 30 to 120 days. Samples 3 and 4 reveal a decrease in pit depth mode with time, which is implausible and most likely a result of sampling statistics.

Maximum Pit Depth. There is a general trend for maximum pit depths to occur in regions containing the smallest percentage of pit area, specifically in the beam areas (Figure 12). This is true in Samples 3-5. The deepest pitting in Sample 1, however, occurs in the ring of corrosion just outside the beam treated area. There is a large macroscopic pit in this ring which is orders of magnitude deeper than any other pit observed.

The central beam areas of Samples 1-3 perform much better than the control with regards to maximum pit depths in these regions. In view of kinetics, the pits in the beam area of Sample 3 demonstrate the greatest stability, where the pits in Samples 1 and 5 appear to be growing at a very rapid rate.

Final Assessment

The overall performance of the ion beam treatments was determined by ranking the samples in three categories: (a) the average "pit area" data in the central beam region (Table 2), (b) the maximum pit depth in the central beam region (Table 4), and (c) the UVAPP in the central beam region (Table 5). Pit depth mode data was not considered because it did not exist for every sample.

The data in Table 5 is proportional to the volume of material lost in the pitting corrosion process. This data was calculated on a frame-by-frame basis, so that when there was only one pit (no depth mode available), the data for this frame was simply the pit depth (maximum pit depth) of that particular pit multiplied by the percent pitted area corresponding to that pit.

Samples were ranked according to performance relative to the control sample (Sample 6), as well as to the kinetics of pit development (i.e., the percent change from 30 to 120 days). Only the 120-day data were used to compare sample treatments to the control.

Once ranked in order of performance, the sample treatments were assigned a score of from 1 through 5 (5 is the best) in each of the three categories. The results are shown in Table 6. A second assessment was made simply on the calculated percentages themselves with the intention of providing a more precise ranking. This is shown in Table 7.

By ranking the treatments from 1 to 5, the best corrosion performance is observed in Sample Treatment 3 (H^+ beam into butadiene), followed by Sample Treatment 2. Samples 4 and 5 received the same score. The more refined analysis again showed Sample Treatment 3 as the best, but Sample Treatment 5 outperformed Treatment 4. Based on these results, both Sample Treatment 3 and Sample Treatment 2 (ethylene beam only) consistently perform better than the other ion beam processes and show the most promise in improving the corrosion behavior of aluminum in seawater.

DISCUSSION

The tendency of a coated metal to corrode is dependent on three factors: (a) the nature of the substrate, (b) the character of the interfacial region between the coating and the substrate, and (c) the nature of the coating.¹⁷ Interest in monomer ion implantation has stemmed from its ability to affect all three of these factors and, in particular, the interfacial region.

The process of monomeric ion implantation incorporates topics such as atomic collision theory, bonding theory, film formation, and adhesion; consequently, many questions may arise with regards to the elemental depth profiles, the chemical and

electrical properties of the film, and the mechanism of ion/substrate interaction. These matters will be the topic of future experimentation. The intent of this study was to examine the practical application of these novel plasma-based films for their ability to protect an alloy in a corrosive environment. The organic films examined were formed by three basic methods: monomer beam implantation, collisional implantation, and plasma polymerization.

As mentioned, monomer ion implantation can affect the substrate, the film, and the film/substrate interface. Therefore, the discussion will be broken down according to these topics for convenience.

EFFECT OF ION IMPLANTATION ON THE SUBSTRATE

The atomic collision theory of Lindhard^{18,19} has been applied in the general treatment of low-energy ion/matter interactions. Although the complexity of monomeric ions and their corresponding collision processes precludes the development of an accurate collision model, there are some general features common to most implantation processes which may help in understanding the process of monomeric ion implantation.

Singly ionized monomer molecules are produced in the ion source via the collision between excited free electrons (generated by a tuned radio frequency) and the monomer gas molecules. These positive monomeric ions are then pushed out of the ion source (by a positively biased probe), accelerated (30 keV), and focused into a beam which typically has a gaussian-shaped energy distribution. Therefore, in the most simple case of an ion beam with no collisional gas, one would expect a central area of intense treatment which tapers off as one moves to the sample perimeter.

A monomer ion with a kinetic energy of 30 keV has four orders of magnitude more energy than the binding energy of a C-C or C-H bond.²⁰ Therefore, when this molecule impacts against the substrate, these bonds are broken and the carbon and hydrogen atoms implant as individual moieties.

As an energetic atom penetrates into the target material, it initiates a large number of atomic collisions in the material, forming a collision cascade. Collisions in the near-surface region can lead directly to sputtering. Collisions inside the material can result in atomic mixing due to recoil implantation, radiation-defect-enhanced diffusion, and thermal spike effects.²¹ The result of ion implantation

is the formation of a surface alloy of graded composition that poses no well-defined interface with respect to the substrate, as does the deposited layer formed in ion plating (e.g., plasma polymerization). Elemental depth profiles on silver targets using SIMS have shown that a 30-keV ethylene beam produces carbon penetration to an approximate depth of 150A and hydrogen penetration to an approximate depth of 1000A. Due to the self-reactivity of the monomer ions, a 30A film is also formed. The ratio of carbon to hydrogen in this film is the same as the implant gas. The attractiveness of this implantation process relies on the possible reestablishment of bonds between the carbon and hydrogen in the substrate and the carbon and hydrogen in the film.

Implantation of an energetic elemental species into a metal has the potential to produce several alterations in the target surface: increased oxide thickness, amorphization, and a carbon contamination film. All of these can have some effect on the corrosion characteristics of the substrate material.

Enhanced oxide growth is almost a universal feature to the ion implantation process, and improved corrosion resistance has been attributed to this phenomenon.⁷ Another possible mechanism for improved corrosion resistance is amorphization of the surface region. When either the host or the implanted species is nonmetallic, then damage effects are more prominent due to anisotropy of bonding.²⁰ As the ion dose increases, stresses in the implant layer increase, which results in the increase of the dislocation density. Eventually, a point is reached where the surface is essentially amorphous with few or no inhomogeneities. Although improved corrosion resistance has been noted in amorphous metals,²² some feel that the damage introduced into the surface layers by ion implantation is insufficient to effect the corrosion reaction.^{7,23}

All electron and ion beam processes are subject to the potential of hydrocarbon contamination, which can lead to carbon layer formation.²¹ It is unclear what effect this may have on the corrosion behavior of a metal.

Sample Treatment 1 (30-keV H⁺ beam) displayed improved corrosion behavior in the beam-treated region, which may have been a result of one or a combination of the mechanisms just described (i.e., oxide enhancement, amorphization, contaminant

film production). So in essence, the hydrogen beam functioned as a processing control. The appearance of the annular region of corrosion around the beam-treated area may be due to the cathodic nature of the beam area driving the unprotected region around it. There is also the possibility of sputtering some of the aperture material into the fringes of the beam area, resulting in an alloy with galvanic activity. However, no tantalum aperture material was detected in this region using energy dispersive x-ray microanalysis. As already mentioned, there is a gaussian-type distribution of energy across the beam cross section. It is possible that beyond a certain point in the beam cross section, there is insufficient energy to produce the oxidation or amorphization of the surface necessary to protect the metal.

The ability of an organic coating to protect a metal substrate from corrosion is primarily a function of two factors: (a) the barrier properties of the coating, and (b) the ability of the film to adhere to the substrate in the presence of water. If a film provides a barrier to the reactants, i.e., water, oxygen, and ions, the corrosion process cannot proceed. Organic coatings are not total barriers to these species; therefore, the most critical consideration in formulating a coating for corrosion protection is to assure interfacial adhesion in the presence of water and hydroxyl ions.²⁴

THE METAL/FILM INTERFACE

Film integration into the substrate aluminum can be accomplished by direct implantation of the atomic series or by recoil implantation in atomic mixing.²¹ This latter process could be the potential mechanism for film stabilization in the collisional implantation processes. It is also possible that the production of lattice imperfections (i.e., vacancies, dislocations, and stacking faults) by ion bombardment will enhance the transport of surface film atoms into the substrate and contribute to the adhesion of the film.⁹

Pits which formed under the plasma polymerized films (outer regions of Sample 3, 4, and 5) formed "channels" whereby pits developed interconnecting paths similar to filiform corrosion (a form of blistering²⁴). Filiform corrosion (and blistering) is a result of poor film adhesion. The strong attractive forces of water to the metal

oxide surface are greater than the dispersion forces between the C-H groups of the film and metal oxide.²⁴ The pits which formed in the implanted regions of all samples studied did not reveal undercutting and remained as isolated pits, which suggests improved adhesion. The issue of cathodic delamination has not been considered because of the poor reactivity of the aluminum oxide surface for the oxygen reduction reaction.

THE FILM

The properties of a polymeric coating depend not only on the size, shape, and chain structure of the individual units, but also on the spatial shape of the polymer molecules.¹⁷ Through thermal motion of the polymer molecules, points of water and electrolyte passage are inherent. This is in addition to the fact that the high osmotic pressure which drives water into an organic film²⁵ makes the production of an impermeable barrier very difficult.

When water and oxygen (or H^+) reach the substrate, corrosion begins. The corrosion reactions result in the formation of soluble ionic products dissolved in the water at the interface. Osmotic forces cause additional water to permeate and, if the coating adhesion is insufficient, a blister will form. This is somewhat suppressed for the ion-implanted coatings because of the elimination of the interface. The barrier properties of the coatings can be further improved by increasing the diffusion path for the reaction species by increasing the film thickness or addition of fillers, by increasing the cross-link density, or by producing films which can resist hydrolysis.^{17,24} The reduced blister formation in the beam-treated areas may be a result of radiation-enhanced cross linking (in addition to, or independent of, improved adhesion). An osmotic cell under a highly cross-linked film will not expand due to the higher rigidity of the cross-linked polymer. The pressure inside the cell will resist the osmotic pressure, and net diffusion stops.²⁴

There is reduced pitting (with regard to pit area) in the beam-treated areas of all samples (1, 3, 4, and 5) when compared to the control sample. One must consider two possible effects other than the ion treatment itself. That is, is the reduced pitting a result of a sacrificial anode effect where the increased corrosion in the

outer region is protecting the central area? Or is the reduced pitting in the beam area a result of increased film thickness in these regions? If the outer region were operating as a sacrificial anode, then one would not expect the increase in the maximum pit depth observed in the beam treated area in these samples (Figure 12). There is certainly some variation in film thickness as one traverses the sample. One would expect a gaussian-type curve, with the thickness tapering off as one went radially out from the center of the sample. Therefore, the pit area should be an inverse of this curve since the diffusion of reacting species is inversely related to thickness. This phenomenon is observed in Sample 4 (see Figure 7); however, Samples 3 and 5 show a sharp increase in pit area beyond the beam area. The differences in these regions (beam vs. outer region) are probably more a function of polymer structure (i.e., molecular weight and crosslink density). Film characterization with respect to thickness and chemical properties are presently underway.

CONCLUSION

The technique of monomer ion implantation has been demonstrated as a viable process for producing corrosion-resistant organic films. In particular, films produced by the collision of a 30-keV H^+ beam into 1,3 butadiene, and those produced by a 30-keV ethylene beam, provide the best protection of the ion beam techniques screened. Inferior barrier and adhesion properties of ion-plated films resulted in poor corrosion resistance in comparison to films formed by the implantation process. Some corrosion resistance was provided by a 30-keV H^+ beam treatment; however, this protection diminished rapidly with time.

Monomer ion implantation provides the flexibility and potential to perform a multitude of surface treatments. Along with this flexibility, however, come many processing variables. This investigation was not intended as an examination of the participating operational variables, nor was it an examination of the solid-state interactions between implant and target species. In addition to processing mechanisms, questions exist as to the mechanism of corrosion protection provided by these organic films. That is, what are the roles of the barrier properties and adhesion of these films in their ability to protect a metal surface? The answers to these questions can only be provided by future experimentation.

SUGGESTED FUTURE WORK

The electrical properties of these ion-beam-related polymer films should be analyzed. The pure resistance of polymer coatings can be related to their ability to protect metal substrates. Parameters derived from ac impedance measurements can be correlated with ionic permitivities of the films as well as water uptake. Disbonding of films can be determined by changes in slope of complex permitivity vs. log frequency plots. There is also a potential benefit in the reverse direction. A monomerimplanted film may provide a means of better understanding ac impedance responses. There are many situations where it is difficult to determine water distribution in the film, i.e., is the water collecting at the film/substrate interface or is it dispersing in the film? A film which does not possess a classical interface may function as a control in order to separate these effects.

The adhesion of these films needs further investigation. This may be achieved by standard techniques (ASTM D 1654-79a) or by specially designed methods.

The feasibility and potentially large benefits of grafting other polymers onto these monomer implanted films needs to be established.

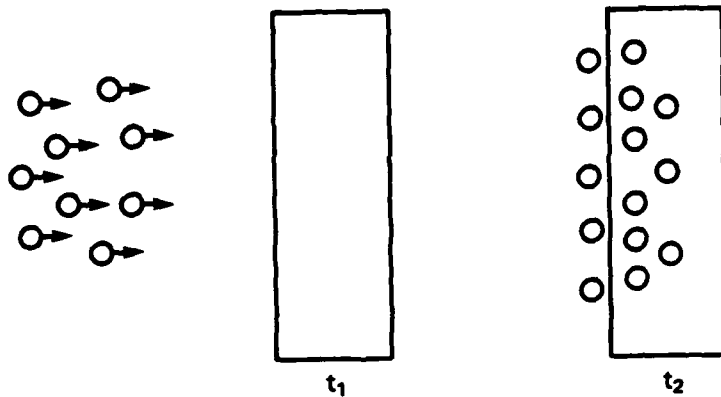
The effect of substrate preparation should be examined. Pre-sputtering prior to implantation may provide a more suitable surface for ion/substrate interaction. This can be compared with natural oxides and anodically produced oxides.

The possibility exists of forming fluorocarbon films by the monomer implantation process. This has the potential to provide superior barrier properties, as well as improved friction and chemical stability.

The effect of individual C and H beams together must be analyzed and compared with monomer beams in their effect on corrosion properties.

The effect of variations of important beam parameters, such as accelerating voltage, target bias voltage, time, collisional gas partial pressure, etc., must be vigorously investigated.

BEAM IMPLANTATION:



COLLISIONAL IMPLANTATION:

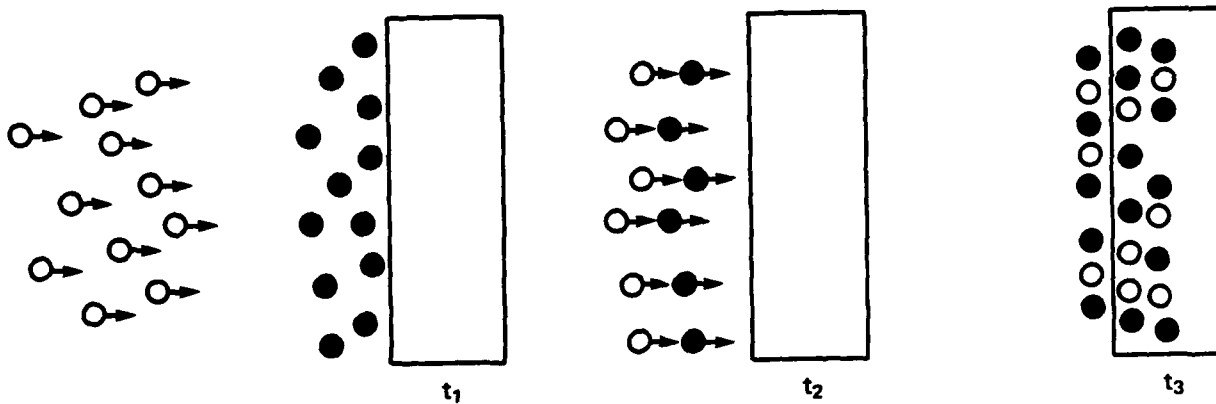


Figure 1 - Implantation Modes

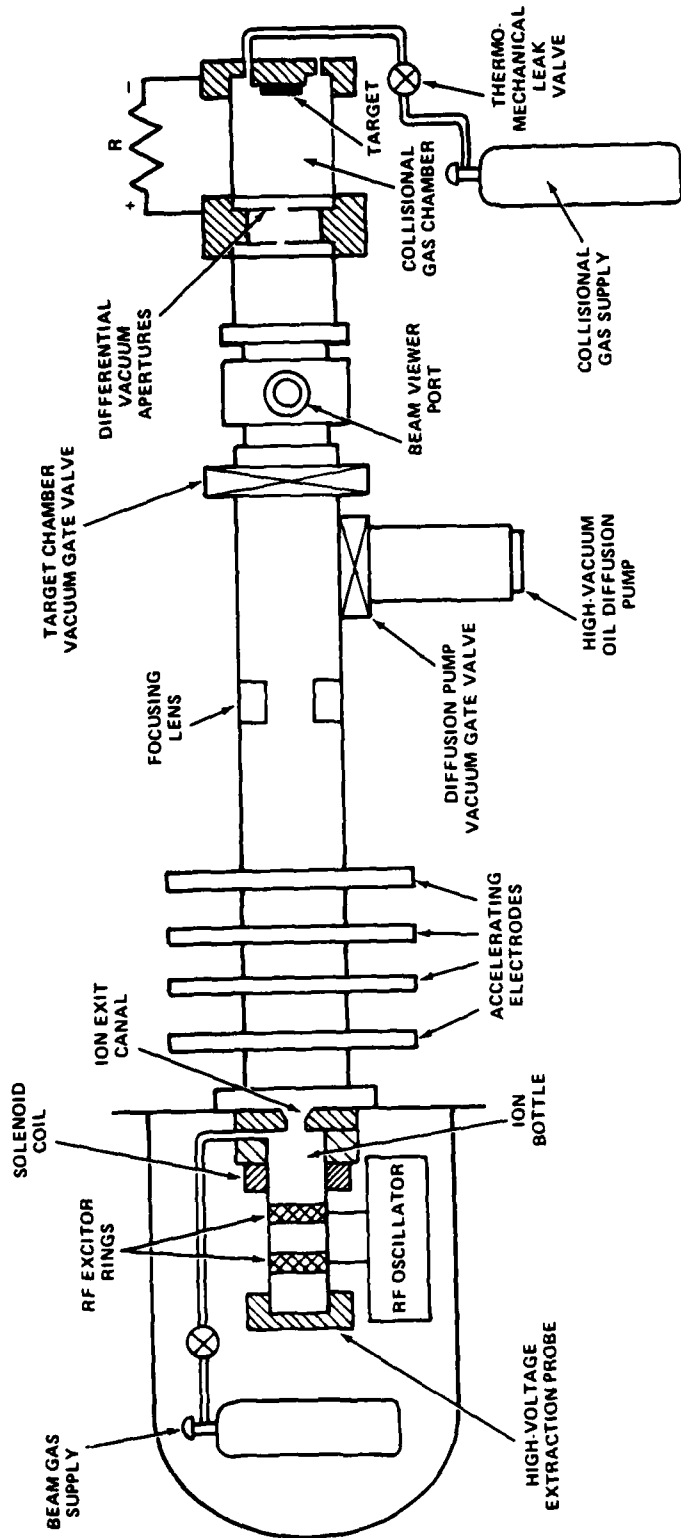


Figure 2 - Schematic of Ion Implantation Device

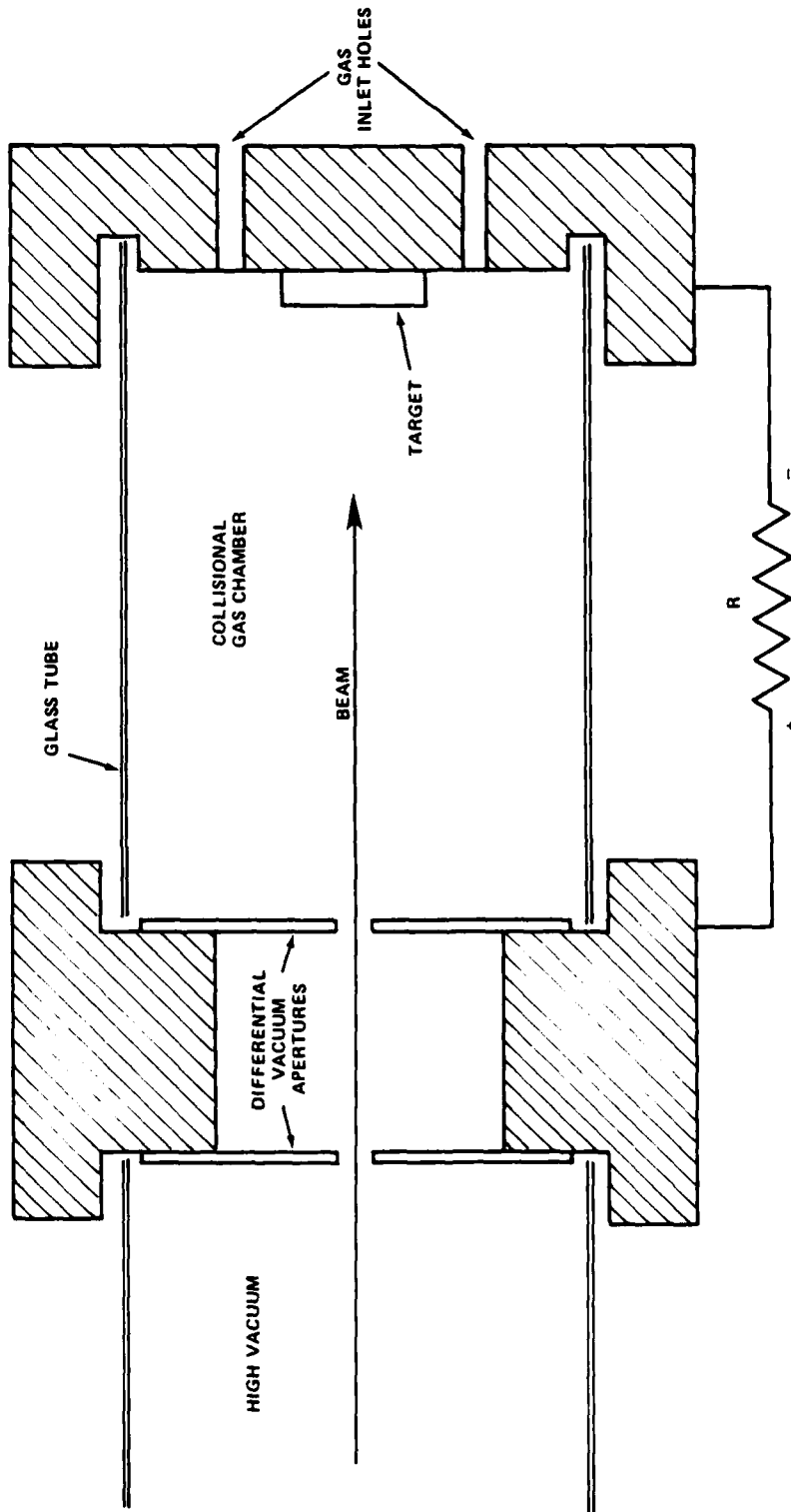
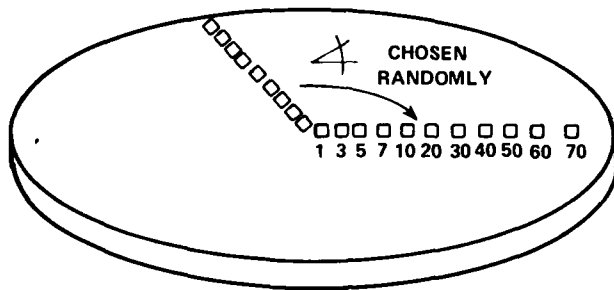


Figure 3 - Differentially Pumped Collisional Gas Chamber



$$\text{PERCENT PIT AREA} = \frac{\text{SHADED AREA}}{A \times B} \times 100$$

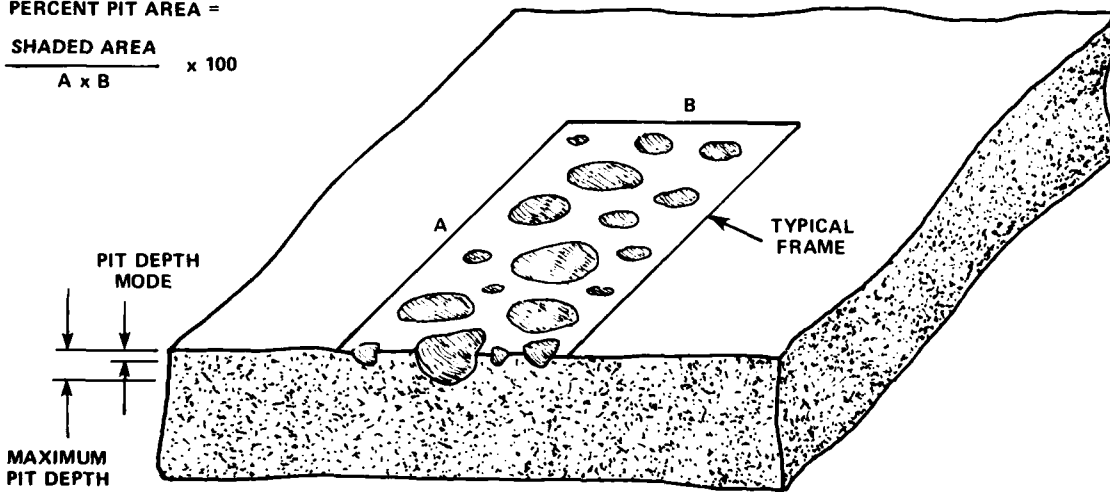
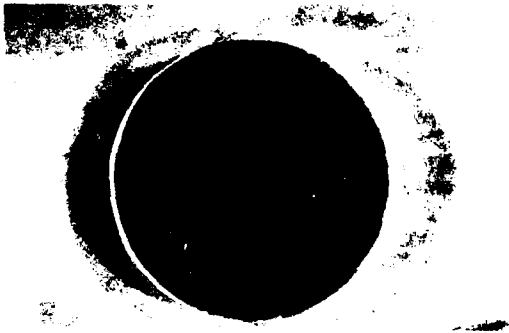


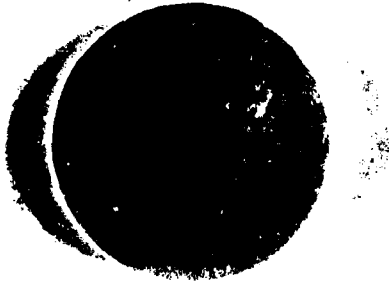
Figure 4 - Sampling Schemes Used to Assess Specimen Corrosion



TREATMENT 1



TREATMENT 2



TREATMENT 3



TREATMENT 4



TREATMENT 5



CONTROL

Figure 5 - Appearance of Typical Sample Treatments and Control Specimen Before Corrosion Testing (1-in.-diam discs)



Figure 6a - Specimen Upon Seawater Removal



Figure 6b - Specimen After Light Mechanical Cleaning

Figure 6 - Sample Treatment 4 After 120 Days of Seawater Immersion

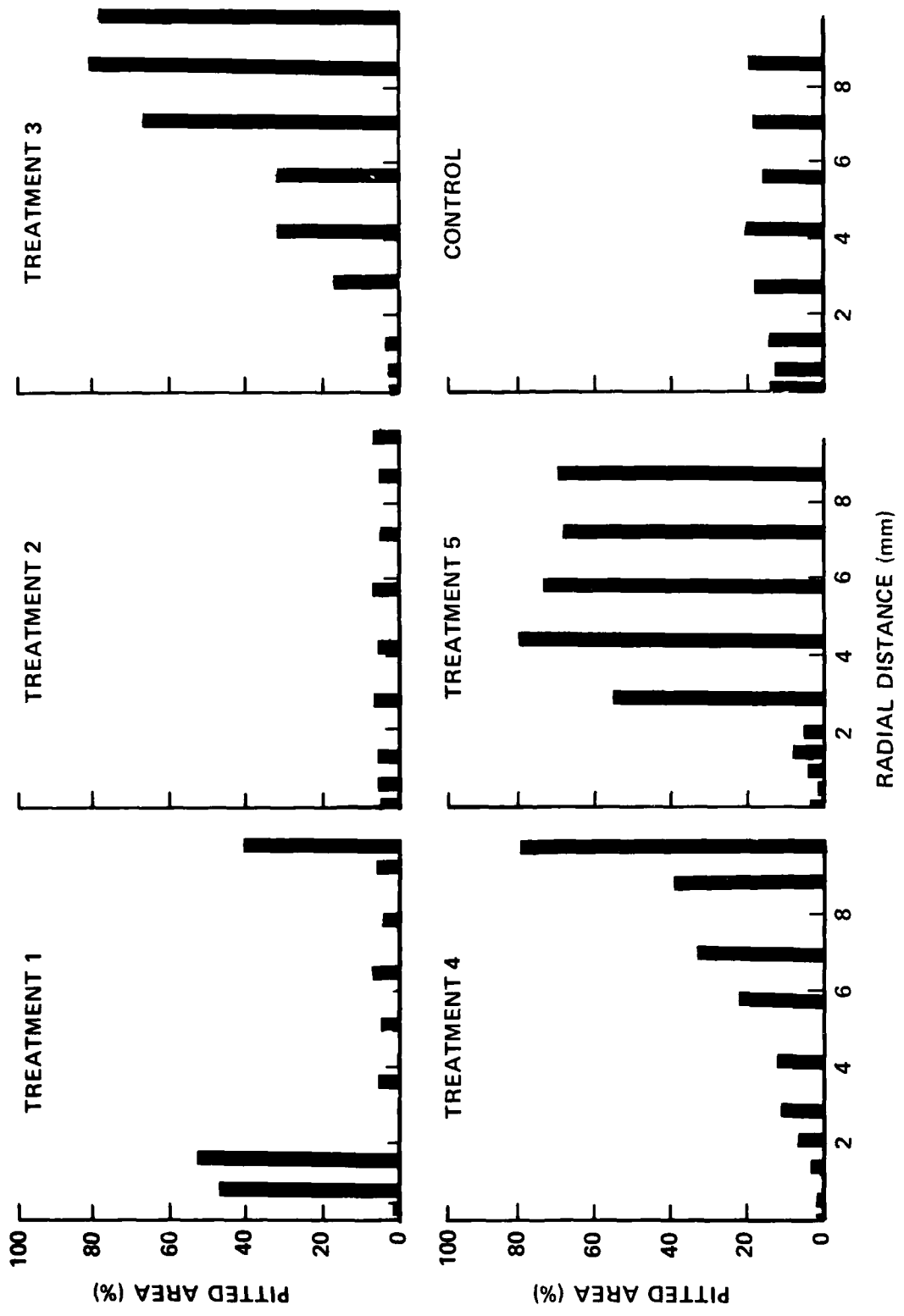


Figure 7 - Percent Pitted Area for 30-Day Exposure

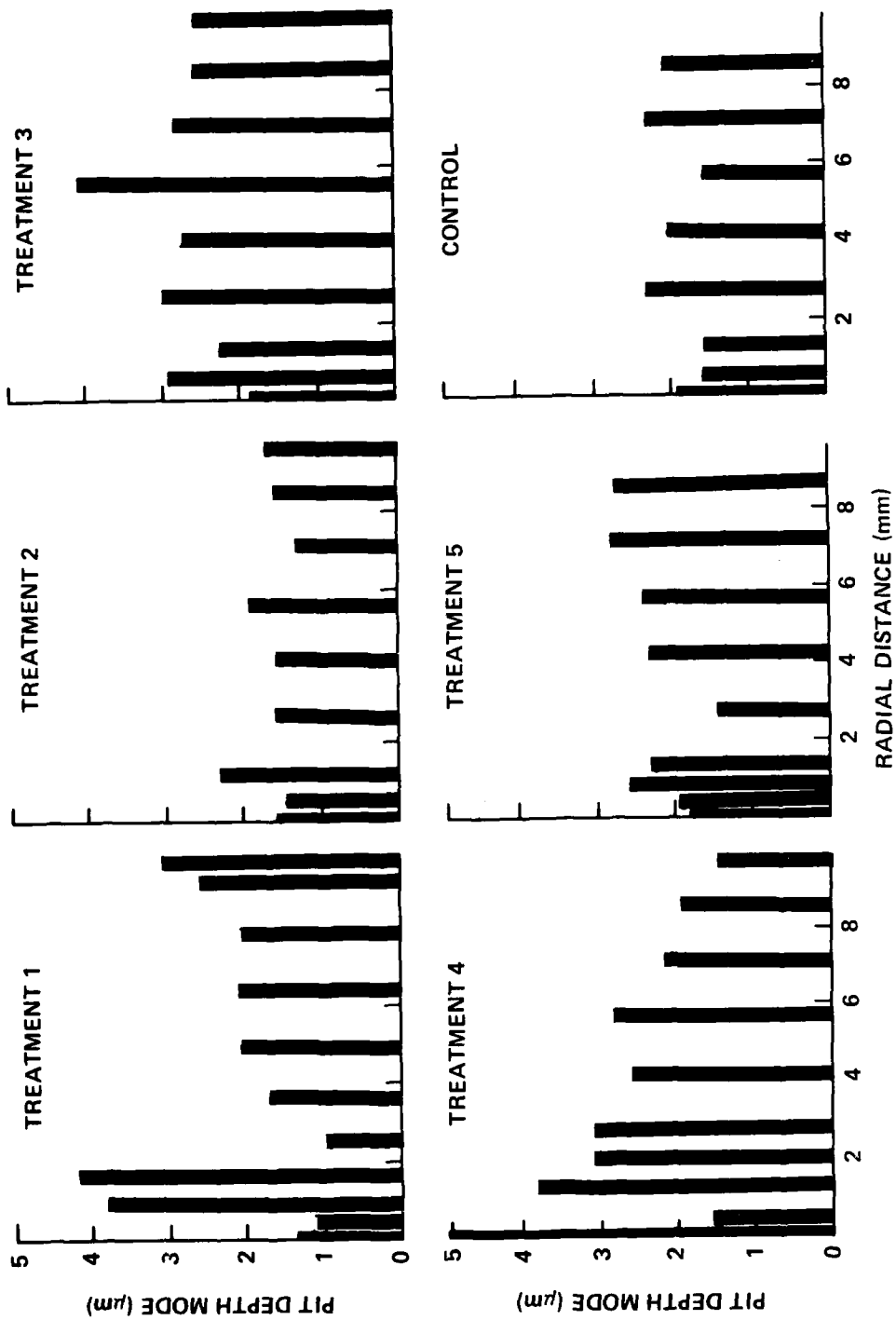


Figure 8 - Pit Depth Mode for 30-Day Exposure

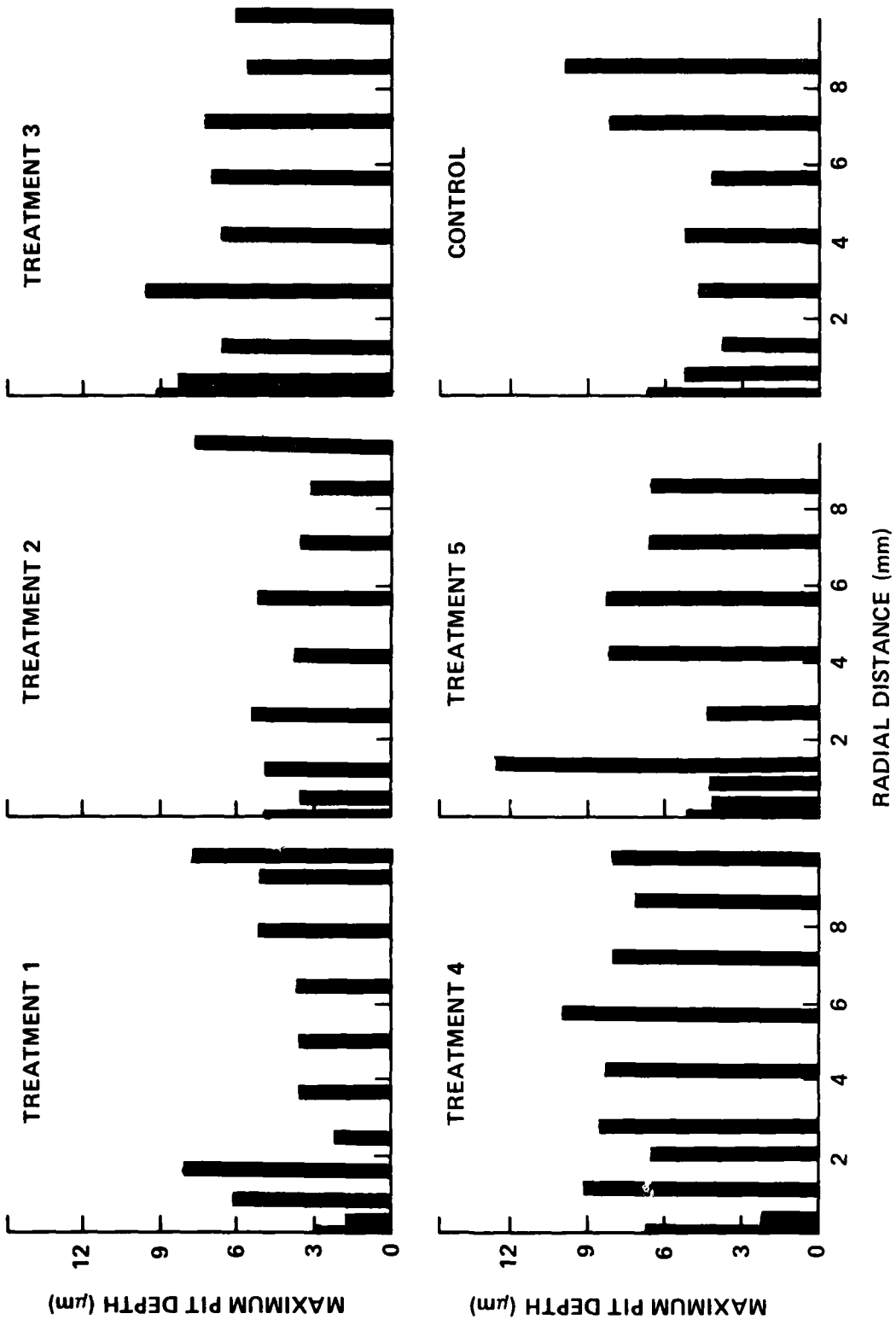


Figure 9 - Maximum Pit Depth for 30-Day Exposure

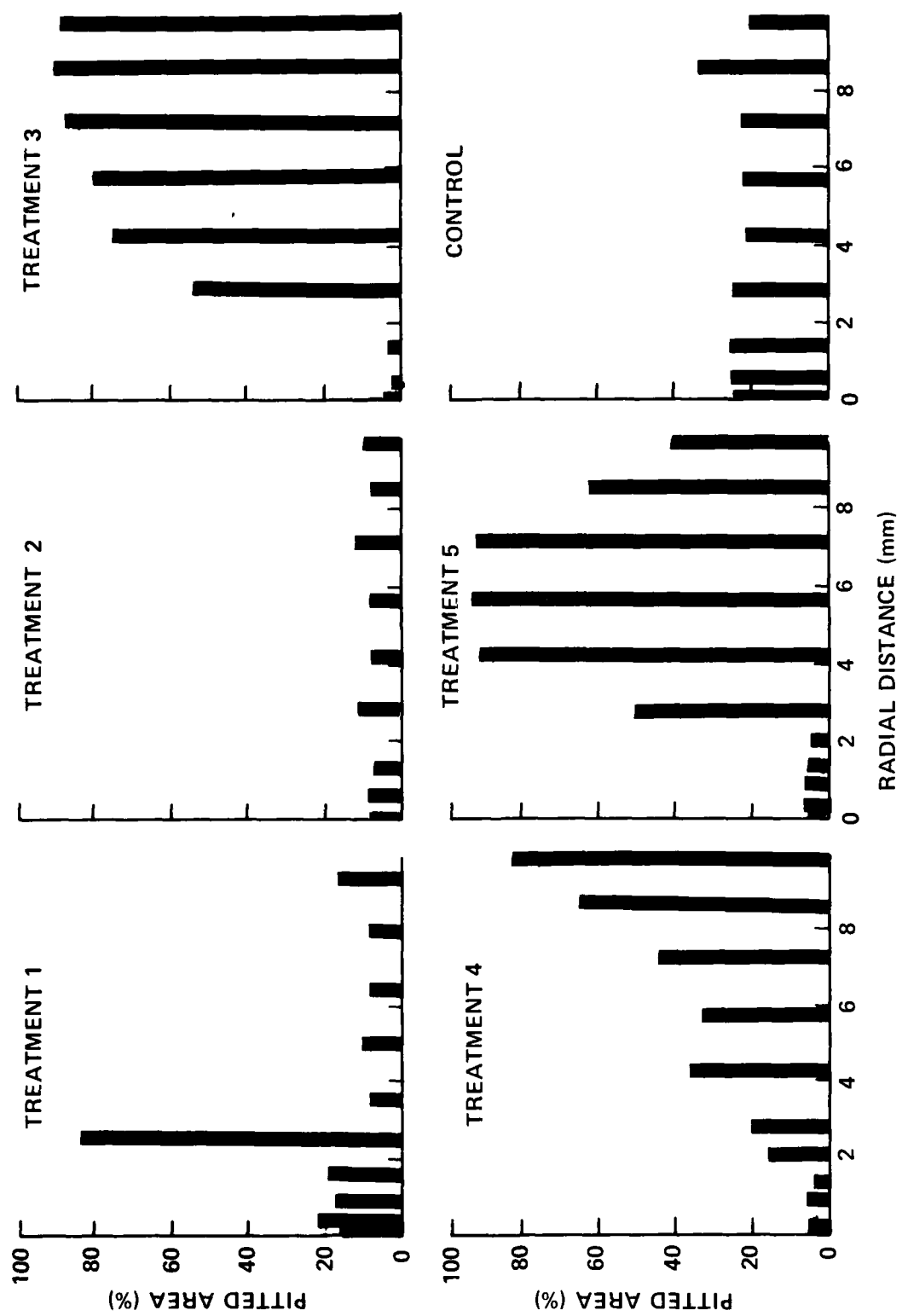


Figure 10 - Percent Pitted Area for 120-Day Exposure

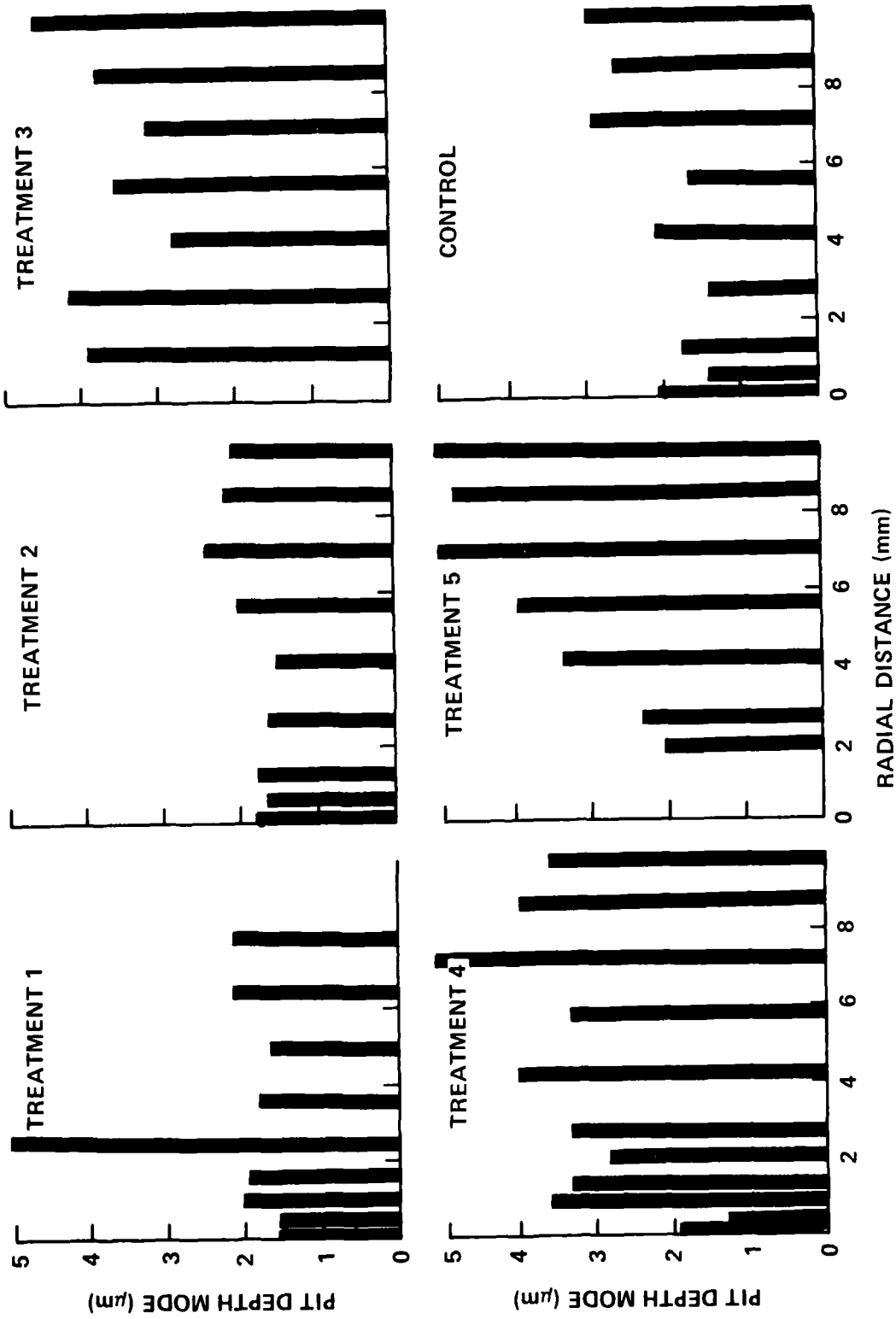


Figure 11 - Pit Depth Mode for 120-Day Exposure

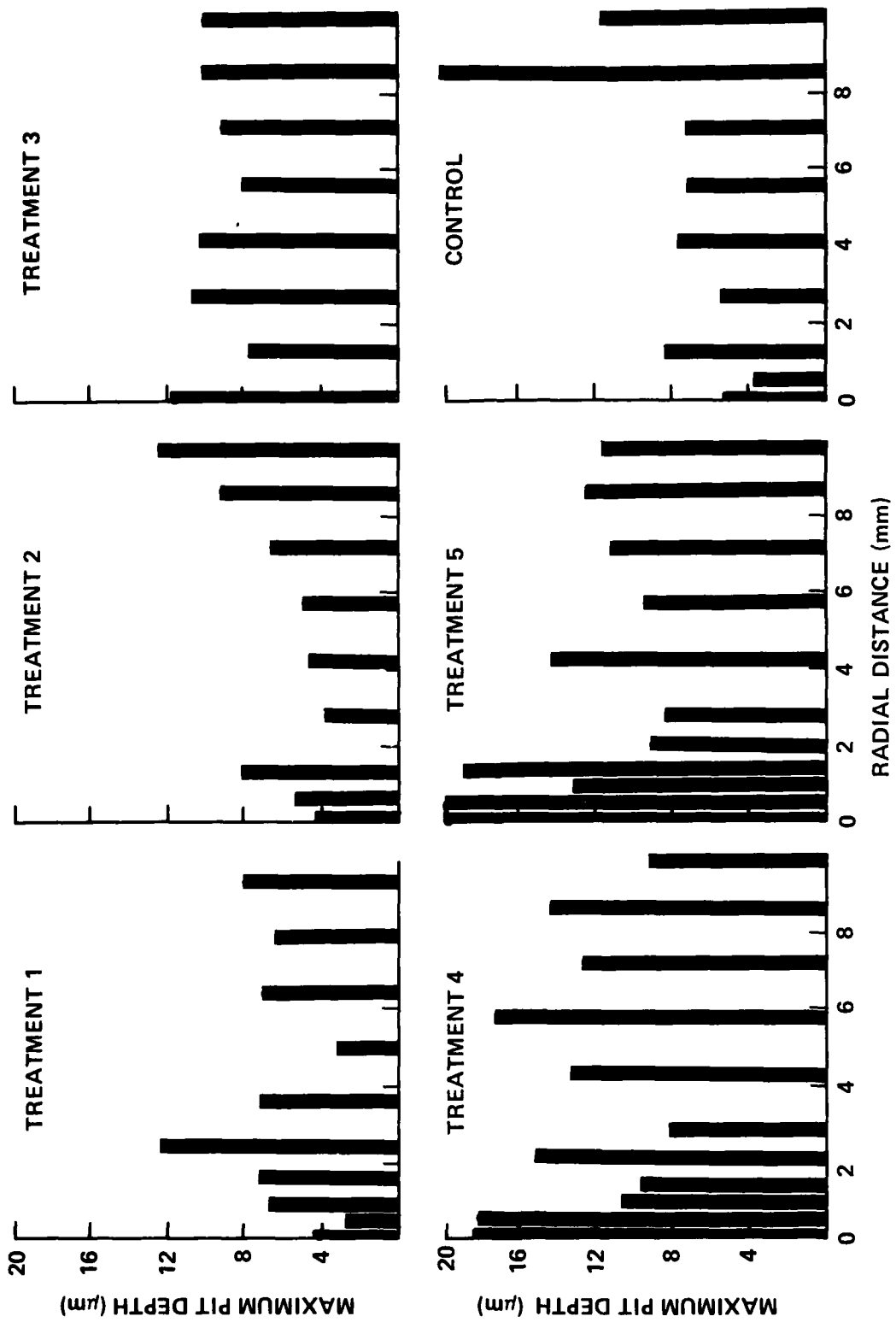
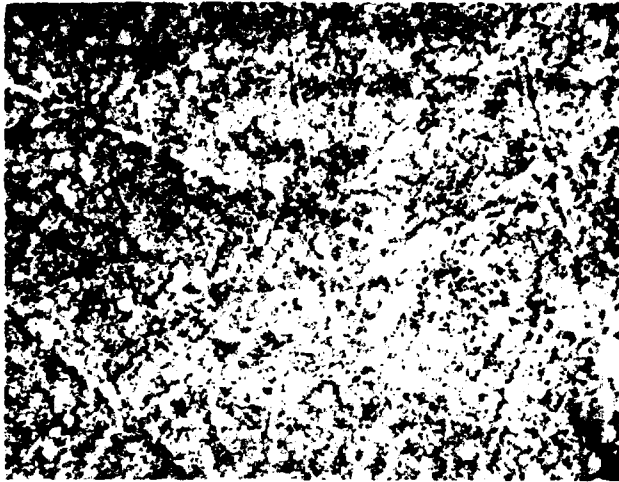
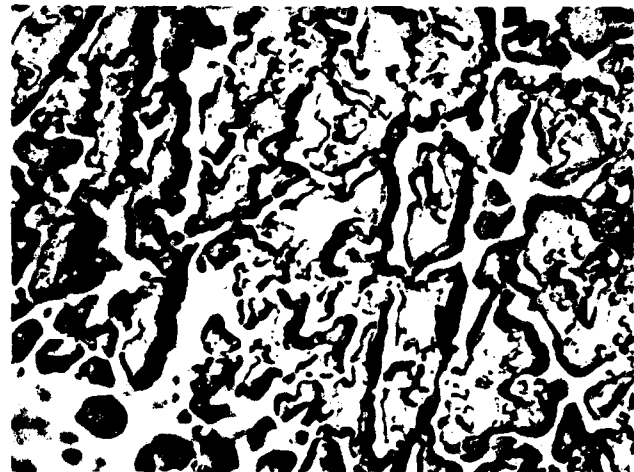


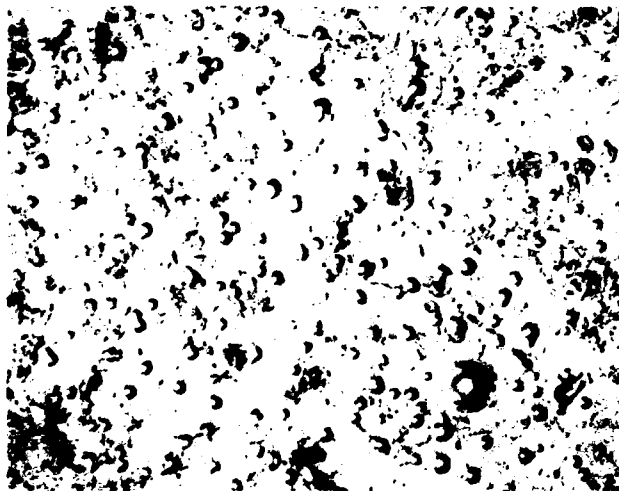
Figure 12 - Maximum Pit Depth for 120-Day Exposure



CENTRAL BEAM AREA (450X)



ANNULAR REGION OF CORROSION
JUST OUTSIDE OF THE BEAM
AREA (450X)

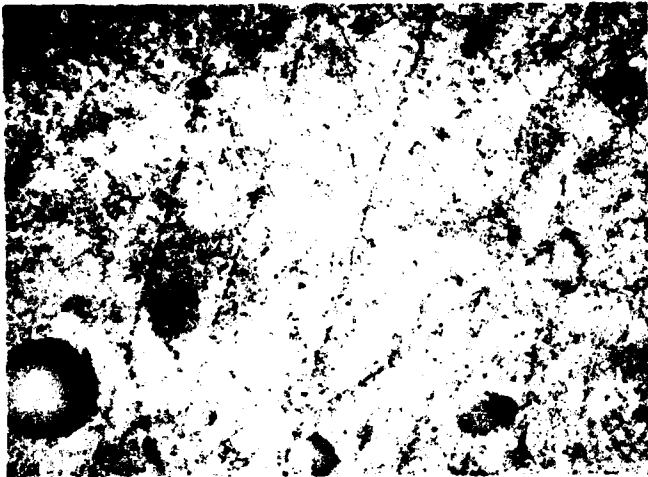


OUTER REGION (450X)

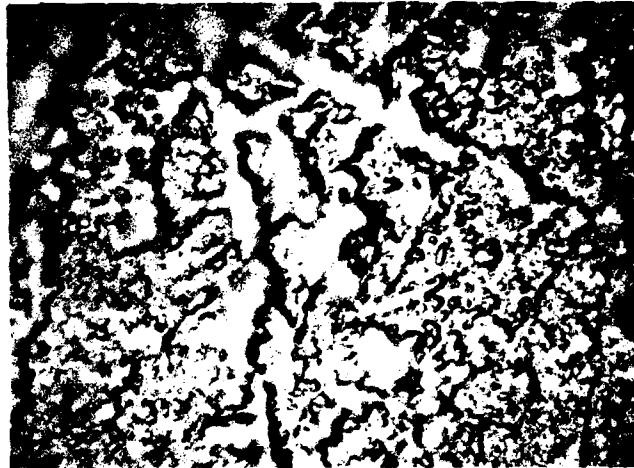
Figure 13 - Sample Treatment 1 After 120-Day Exposure



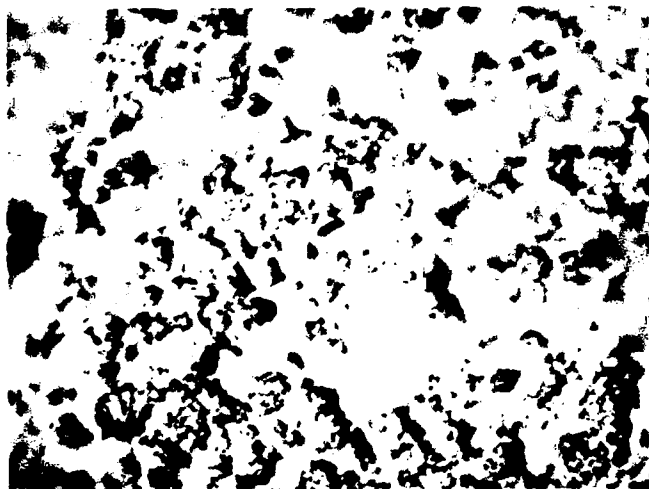
Figure 14 - Typical Pitting on Sample Treatment
2 After 120-Day Exposure (450X)



CENTRAL BEAM AREA (450X)

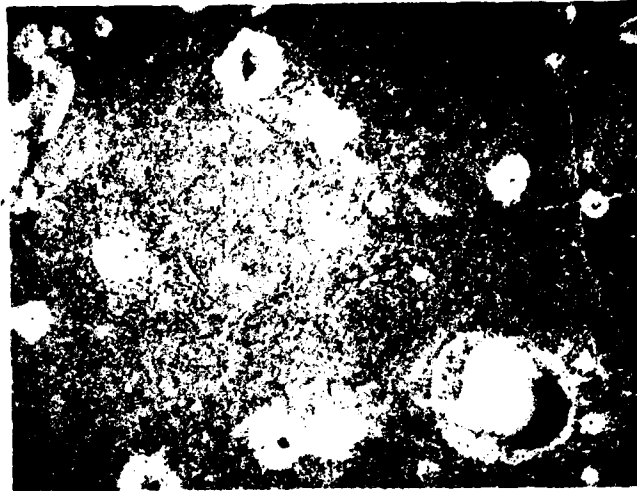


REGION AT PERIMETER OF ION
BEAM AREA (450X)

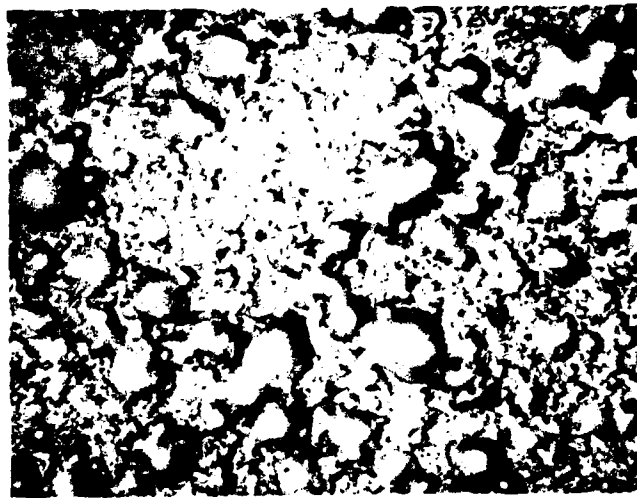


OUTER REGION (450X)

Figure 15 - Sample Treatment 3 After 120-Day Exposure

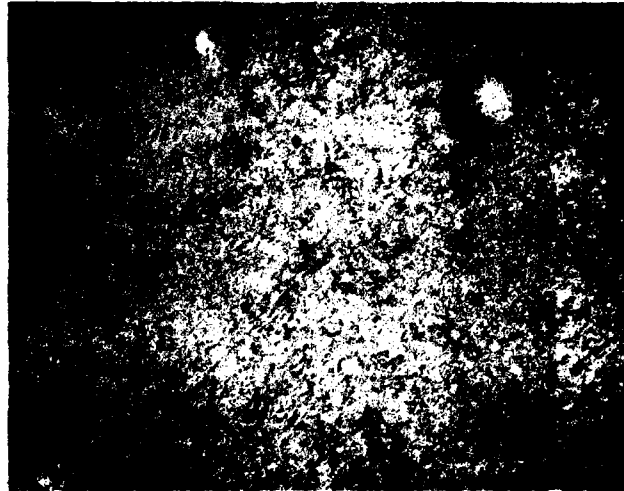


CENTRAL BEAM AREA (450X)

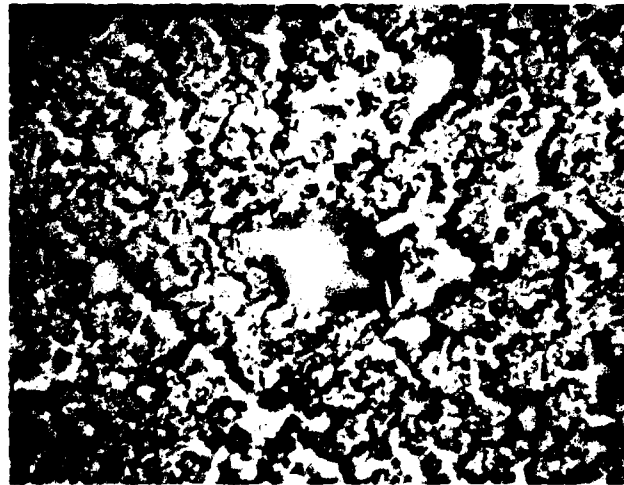


OUTER REGION (450X)

Figure 16 - Sample Treatment 4 After 120-Day Exposure

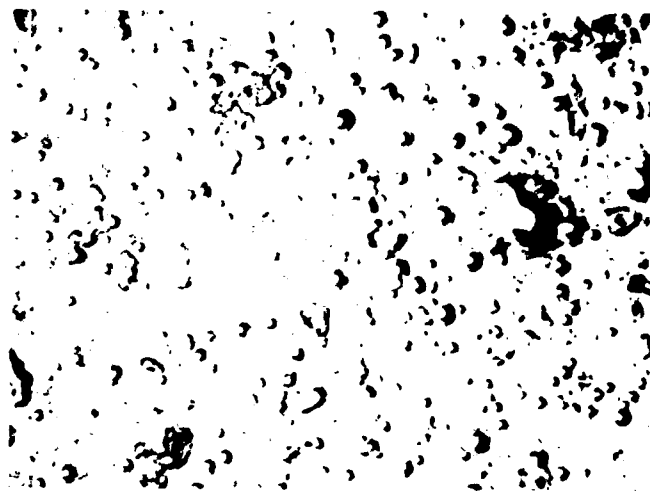


CENTRAL BEAM AREA (450X)



OUTER REGION (450X)

Figure 17 - Sample Treatment 5 After 120-Day Exposure



TYPICAL PITTING (450X)

Figure 18 - Control After 120-Day Exposure

TABLE 1 - SUMMARY OF SAMPLE TREATMENTS

Sample Treatment	Beam Gas	Beam Energy (keV)	Apertures	Collisional Gas	Target Bias (V)
1	H ⁺	30	Yes	--	--
2	Ethylene	30	No	--	--
3	H ⁺	30	Yes	1,3 Butadiene	136
4	H ⁺	30	Yes	1,3 Butadiene	1000
5	Ethylene	30	Yes	1,3 Butadiene	90
6	Control Set				

TABLE 2 - COMPARISON OF SAMPLE TREATMENTS AS TO AVERAGE PERCENT PITTED AREAS AFTER TWO IMMERSION PERIODS

Sample Treatment	Region of Interest	30 Days		120 Days		Change From 30 to 120 Days (%)
		Pitted Area (Avg. %)	Compared to Control Pit'g. (%)	Pitted Area (Avg. %)	Compared to Control Pit'g. (%)	
1 (H ⁺ Beam Only)	Beam Area	2.5	16.3	17.2	73.9	588
	Outer Area	10.4	68.1	22.5	96.4	116
2 (Ethylene Beam Only)	Treatment Area*	4.6	30.1	7.9	33.7	71
3 (H ⁺ Beam Into Butadiene)	Beam Area	2.2	14.2	1.3	5.7	--
	Outer Area	44.2	288.9	75.5	324.4	71
4 (H ⁺ Into Butadiene Plus Glow Discharge)	Beam Area	0.7	4.4	4.1	17.6	507
	Outer Area	18.3	119.9	34.5	148.2	88
5 (Ethylene Into Butadiene)	Beam Area	2.5	16.3	4.0	17.2	60
	Outer Area	67.4	440.4	76.0	326.6	13
6 (Control)	--	15.3	--	23.3	--	52

*Sample treatment 2 covered the entire specimen surface.

TABLE 3 - COMPARISON OF AVERAGE PIT DEPTH MODE

Sample Treatment	Region of Interest	30 Days		120 Days		Change From 30 to 120 Days (%)
		Pitted Area (Avg. %)	Compared to Control Pit'g. (%)	Pitted Area (Avg. %)	Compared to Control Pit'g. (%)	
1 (H ⁺ Beam Only)	Beam Area	1.2	61.3	1.7	86.3	50.0
	Outer Area	2.1	113.8	2.8	142.4	25.1
2 (Ethylene Beam Only)	Treatment Area*	1.6	86.6	1.9	93.8	14.7
3 (H ⁺ Beam Into Butadiene)	Beam Area	2.3	122.7	2.0	97.5	--
	Outer Area	2.2	106.4	3.4	173.7	63.3
4 (H ⁺ Into Butadiene Plus Glow Discharge)	Beam Area	2.6	137.3	2.5	124.8	--
	Outer Area	2.6	136.2	3.8	189.9	39.4
5 (Ethylene Into Butadiene)	Beam Area	2.0	106.7	--	--	--
	Outer Area	2.6	136.2	4.8	194.9	43.1
6 (Control)	--	1.9	--	2.0	--	6.4

*Sample treatment 2 covered the entire specimen surface.

TABLE 4 - COMPARISON OF MAXIMUM PIT DEPTH

Sample Treatment	Region of Interest	30 Days		120 Days		Change From 30 to 120 Days (%)
		Pitted Area (Avg. %)	Compared to Control Pit'g. (%)	Pitted Area (Avg. %)	Compared to Control Pit'g. (%)	
1 (H ⁺ Beam Only)	Beam Area	2.8	28.9	7.0	20.6	150.0
	Outer Area	8.0	82.5	12.0	35.3	50.0
2 (Ethylene Beam Only)	Treatment Area*	5.5	56.7	9.1	26.8	65.5
3 (H ⁺ Beam Into Butadiene)	Beam Area	9.0	92.8	11.5	33.8	27.8
	Outer Area	9.5	97.9	10.5	30.9	10.5
4 (H ⁺ Into Butadiene Plus Glow Discharge)	Beam Area	9.0	92.8	18.1	53.2	101.1
	Outer Area	10.0	103.1	15.0	44.1	50.0
5 (Ethylene Into Butadiene)	Beam Area	12.5	128.9	20.3	59.7	62.4
	Outer Area	8.0	82.5	14.0	41.2	75.0
6 (Control)	--	9.7	--	34.0	--	250.5

*Sample treatment 2 covered the entire specimen surface.

TABLE 5 - COMPARISON OF AVERAGE PITTING PARAMETERS (UVAPPS)

Sample Treatment	Region of Interest	30 Days		120 Days		Change From 30 to 120 Days (%)
		Pitted Area (Avg. %)	Compared to Control Pit'g. (%)	Pitted Area (Avg. %)	Compared to Control Pit'g. (%)	
1 (H ⁺ Beam Only)	Beam Area	3.0	10.2	29.5	63.0	882.5
	Outer Area	34.4	117.3	98.8	211.2	187.2
2 (Ethylene Beam Only)	Treatment Area*	7.5	25.6	14.8	31.5	96.6
3 (H ⁺ Beam Into Butadiene)	Beam Area	5.1	17.2	8.5	18.0	67.3
	Outer Area	126.4	431.1	257.2	549.9	103.5
4 (H ⁺ Into Butadiene Plus Glow Discharge)	Beam Area	2.3	7.7	9.6	20.5	325.6
	Outer Area	124.4	424.2	136.7	292.1	9.9
5 (Ethylene Into Butadiene)	Beam Area	5.3	18.2	34.3	73.3	544.1
	Outer Area	158.8	541.6	301.0	643.5	89.6
6 (Control)	--	29.3	--	46.8	--	59.5

*Sample treatment 2 covered the entire specimen surface.

TABLE 6 - RANKING OF OVERALL PERFORMANCE OF SAMPLE TREATMENTS

Sample Treatment	Ranking Categories*						Total Score (Category Rankings)	Final Ranking**
	Avg. Pitted Area		Max. Pit Depth		Avg. UVAPP			
	Compared to Control Pitting (%)	Change from 30 to 120 Days (%)	Compared to Control Pitting (%)	Change from 30 to 120 Days (%)	Compared to Control Pitting (%)	Change from 30 to 120 Days (%)		
1	1	1	5	1	2	1	11	5
2	2	3	4	3	3	4	19	2
3	5	5	3	5	5	5	28	1
4	3	2	2	2	4	3	16	3,4
5	4	4	1	4	1	2	16	3,4

*Categories Ranked: Best = 5, Worst = 1.
 **Final Ranking: Best = 1, Worst = 5.

TABLE 7 - REFINED RANKING OF OVERALL PERFORMANCE OF SAMPLE TREATMENTS

Sample Treatment	Ranking Categories*						Total Score (Category Rankings)	Final Ranking**
	Avg. Pitted Area		Max. Pit Depth		Avg. UVAPP			
	Compared to Control Pitting (%)	Change from 30 to 120 Days (%)	Compared to Control Pitting (%)	Change from 30 to 120 Days (%)	Compared to Control Pitting (%)	Change from 30 to 120 Days (%)		
1	74	588	21	150	63	883	1779+	5
2	34	71	27	66	32	97	327	2
3	6	0	34	28	18	67	153	1
4	18	507	53	101	21	326	1026	4
5	17	60	60	62	73	544	816	3

*Categories Ranked: Percents from Tables 2 Through 5.
 **Final Ranking: Best = 1, Worst = 5.

REFERENCES

1. Chernow, F., J.A. Borders, and D.K. Brice, eds., "Ion Implantation in Semiconductors," Plenum Press, New York (1977).
2. Namba, S., ed., "Ion Implantation in Semiconductors," Plenum Press, New York (1975).
3. Hirvonen, J.K., "Ion Implantation in Tribology and Corrosion Science," J. Vac. Sci. Technol., 15 (5):1622-1668 (1978).
4. Hartley, N.E.W., "Tribological and Mechanical Properties," in "Treatise on Materials Science and Technology," Vol. 18, ed. by J.K. Hirvonen, Academic Press, New York, pp. 321-368, (1980).
5. van der Weg, W.F., D. Sigurd, and J.W. Mayer, in "Applications of Ion Beams to Metals," ed. by S.T. Picraux, E.P. Eernisse, and F.L. Vook, Plenum Press, New York, p. 209 (1974).
6. McCafferty, E., G.K. Hubler, and J.K. Hirvonen, "Corrosion Control by Ion Implantation," from "Proceedings of the 1978 Tri-Service Conference on Corrosion," M. Levy and J. Brown, eds., Metals and Ceramics Information Center, Columbus, Ohio, p. 435 (1979).
7. Ashworth, V., and P.M. Proctor, "The Application of Ion Implantation to Aqueous Corrosion," in "Treatise on Materials Science and Technology," Vol. 18, ed. by J.K. Hirvonen, Academic Press, New York, pp. 176-256 (1980).
8. Spalvins, T., "New Applications for Sputtering and Plating," NASA TM X-73551 (1977).
9. Tsukizoe, T., T. Nakai, and N. Ohmae, "Ion Beam Plating Using Mass Analyzed Ions," J. Appl. Phys. 48 (11):4770-4776 (1977).
10. Aizenberg, S., and R. Chabot, "Ion-Beam Deposition of Thin Films of Diamondlike Carbon," J. Appl. Phys. 42 (7):2953 (1971).
11. Hirvonen, J.K., "Introduction" in "Treatise on Materials Science and Technology," Vol. 18, ed. by J.K. Hirvonen, Academic Press, New York, pp. 1-16 (1980).

12. Winterbon, K.B., "Ion Implantation Range and Energy Deposition Distributions," Vol. 2, "Low Incident Ion Energies," IFI/Plenum Data Company, New York (1975).
13. Ferralli, M.W., "Deposition of Thin Organic Coats by Ion Implantation," U.S. Patent No. 4264642 (1981).
14. Hilliard, J.E., and J.W. Cahn, "An Evaluation of Procedures in Quantitative Metallography or Volume-Fraction Analysis," Trans. Met. Soc. AIME, 221:344-352 (1961).
15. Gladman, T., and J.H. Woodhead, "The Accuracy of Point Counting in Metallographic Investigations," J. Iron and Steel Inst., pp. 189-193 (Feb 1960).
16. Wonnacott, T.H. and R.J. Wonnacott, "Introductory Statistics," 2nd ed., John Wiley and Sons, Inc., New York, p. 169 (1972).
17. Leidheiser, H., Jr., "Corrosion of Painted Metals - a Review," Corrosion-NACE 38:374-383 (1982).
18. Lindhard, J., V. Nielson, and M. Scharff, "Approximation Method of Classical Scattering by Screened Coulomb Fields (Notes on Atomic Collision I.)," Mat. Fys. Medd. Dan. Vid. Selsk. 36:10 (1968).
19. Lindhard, J., "Thomas-Fermi Approach and Similarity in Atomic Collisions," Nat. Acad. Sci.-NRC publ. 1133 (1965).
20. Myers, S.M., "Implantation Metallurgy - Equilibrium Alloys," in "Treatise on Materials Science and Technology," Vol. 18, ed. by J.K. Hirvonen, Academic Press, New York, pp. 51-82 (1980).
21. Liau, Z.L., and J.W. Mayer, "Ion Bombardment Effects on Material Composition," in "Treatise on Materials Science and Technology," Vol. 18, ed. by J.K. Hirvonen, Academic Press, New York, pp. 17-49 (1980).
22. Hashimoto, K., K. Osada, T. Masumoto, and S. Shimodaira, "Characteristics of Passivity of Extremely Corrosion-Resistant Amorphous Iron Alloy," Corr. Sci. 16:71-76 (1976).

23. Poate, J.M., and A.G. Cullis, "Implantation Metallurgy - Metastable Alloy Formation" in "Treatise on Materials Science and Technology," Vol. 1^P, ed. by J.K. Hirvonen, Academic Press, New York, pp. 85-131 (1980).

24. Wicks, Z.W. Jr., "Principles of Formulating Corrosion Control Protective Coatings," in "Corrosion Control by Coatings," ed. by H. Leidheiser, Jr., Science Press, Princeton, pp. 29-34 (1979).

25. Koehler, E.L., "Corrosion Under Organic Coatings," in "Localized Corrosion," NACE publ., pp. 117-133 (1974).

INITIAL DISTRIBUTION

Copies		CENTER DISTRIBUTION		
		Copies	Code	Name
1	ODUSDR&E/J. Persh			
1	OSD (MRA&L)-WR/W.G. Miller	1	28	
2	ONR/P. Clarkin	1	2801	
1	USAME/G.D. Farmer, Jr.	1	2803	
		3	281	
3	AMMRC/A. Levitt	25	2813	
1	US ARO/J. Hurt	1	2814(DAD)	
1	DARPA	10	5211.1	Reports Distribution
		1	522.1	TIC (C)
3	NRL/J. Sedriks	1	522.2	TIC (A)
2	NAVMAT/J.J. Kelly	2	5231	
5	NAVSEA/M. Kinna			
3	SSPO/LCDR F. Ness			
1	NASC/R. Schmidt			
2	NADC/S. Ketcham			
1	NSWC			
1	NUSC/B. Sandman			
1	NOSC/P.D. Burke			
12	DTIC			
2	AFML			
	1 NMD/R.M. Neff			
	1 MB/D.R. Becker			
2	AFML/T. Ronald			
1	NBS/G. Blessing			
1	NASA			
1	MMCIAC			
1	Aerospace Corporation/W. Riley			

DTNSRDC ISSUES THREE TYPES OF REPORTS

1. DTNSRDC REPORTS, A FORMAL SERIES, CONTAIN INFORMATION OF PERMANENT TECHNICAL VALUE. THEY CARRY A CONSECUTIVE NUMERICAL IDENTIFICATION REGARDLESS OF THEIR CLASSIFICATION OR THE ORIGINATING DEPARTMENT

2. DEPARTMENTAL REPORTS, A SEMIFORMAL SERIES, CONTAIN INFORMATION OF A PRELIMINARY, TEMPORARY, OR PROPRIETARY NATURE OR OF LIMITED INTEREST OR SIGNIFICANCE. THEY CARRY A DEPARTMENTAL ALPHANUMERICAL IDENTIFICATION.

3. TECHNICAL MEMORANDA, AN INFORMAL SERIES, CONTAIN TECHNICAL DOCUMENTATION OF LIMITED USE AND INTEREST. THEY ARE PRIMARILY WORKING PAPERS INTENDED FOR INTERNAL USE. THEY CARRY AN IDENTIFYING NUMBER WHICH INDICATES THEIR TYPE AND THE NUMERICAL CODE OF THE ORIGINATING DEPARTMENT. ANY DISTRIBUTION OUTSIDE DTNSRDC MUST BE APPROVED BY THE HEAD OF THE ORIGINATING DEPARTMENT ON A CASE-BY-CASE BASIS.

END

FILMED

9-84

DTIC